

Cyclopentadienyl Ligands

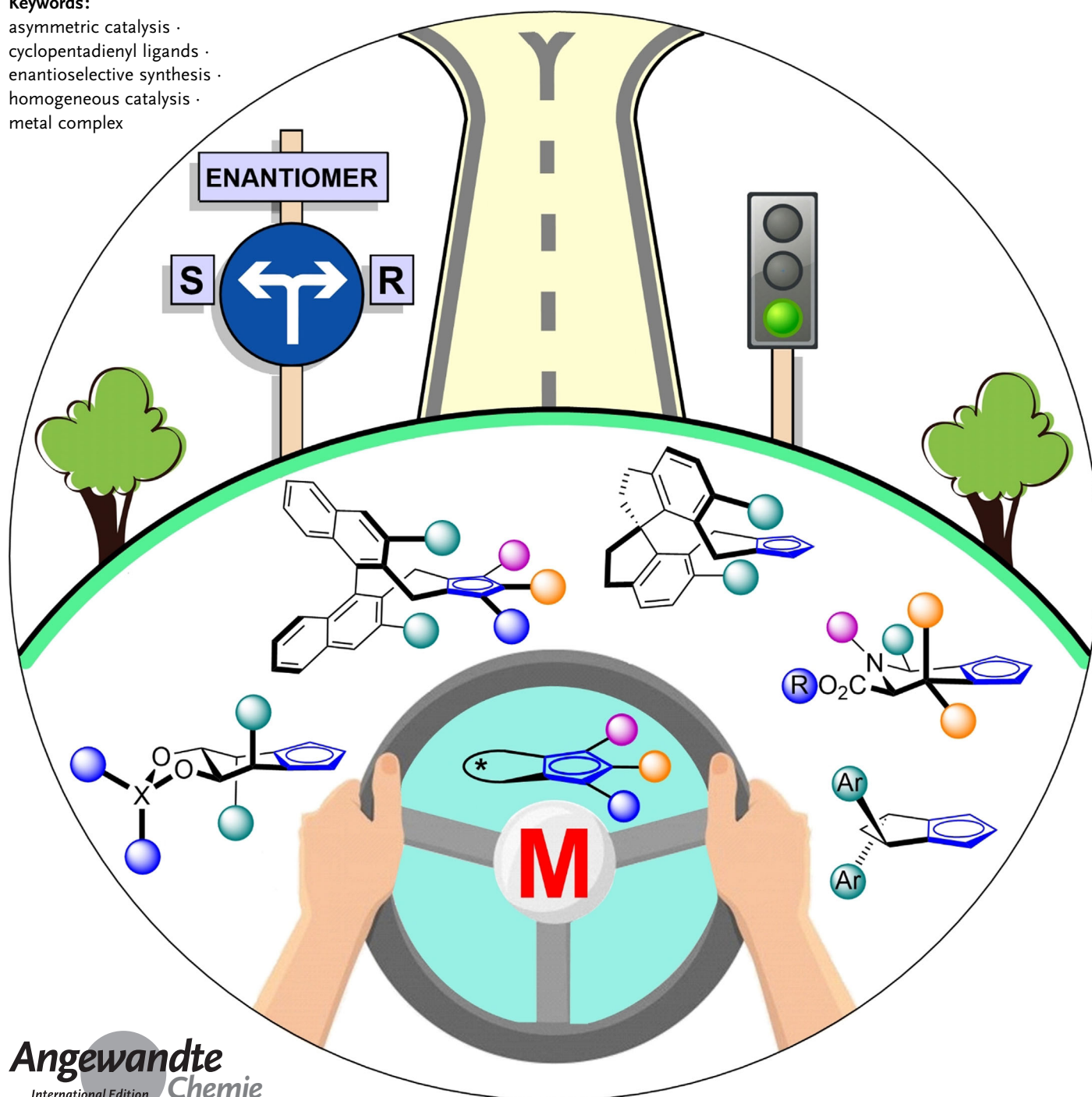
How to cite:

International Edition: doi.org/10.1002/anie.202008166

German Edition: doi.org/10.1002/ange.202008166

Chiral Cyclopentadienyl Ligands: Design, Syntheses, and Applications in Asymmetric Catalysis*Josep Mas-Roselló, Ana G. Herraiz⁺, Benoît Audic⁺, Aragorn Laverny, and Nicolai Cramer****Keywords:**

asymmetric catalysis ·
cyclopentadienyl ligands ·
enantioselective synthesis ·
homogeneous catalysis ·
metal complex



The creation of new chiral ligands capable of providing high stereocontrol in metal-catalyzed reactions is crucial in modern organic synthesis. The production of bioactive molecules as single enantiomers is increasingly required, and asymmetric catalysis with metal complexes constitutes one of the most efficient synthetic strategies to access optically active compounds. Herein we offer a historical overview on the development of chiral derivatives of the ubiquitous cyclopentadienyl ligand (Cp^X), and detail their successful application in a broad range of metal-catalyzed transformations. Those include the functionalization of challenging C–H bonds and beyond, giving access to an extensive catalogue of valuable chiral molecules. A critical comparison of the existing ligand families, their design, synthesis, and complexation to different metals is also provided. In addition, future research directions are discussed to further enhance the performance and application of Cp^X ligands in enantioselective catalysis.

1. Introduction

The production of chiral drugs as their single most desirable enantiomer is becoming a requirement for the chemical industries.^[1] The development of new efficient methods to access enantiopure compounds plays a central role in modern organic synthesis. In particular, asymmetric catalysis with homogeneous metal complexes is one of the most powerful tools to perform highly enantioselective transformations.^[2] The enormous progress achieved in this field is tightly linked to the creation of new chiral ligands that can provide high levels of enantiocontrol and efficiency, being applicable to different reaction systems via the modification of their architectures. Some of the most prevalent ones include TADDOL (**1**), BOX (**2**), BINAP (**3**), BINOL (**4**), and SALEN (**5**) (Figure 1).^[3,4] While these all coordinate to metals through heteroatoms, complementary carbon-coordinating neutral N-heterocyclic carbenes (NHC, **6**)^[5] or cyclopentadienyl anions (Cp^X , **7**)^[6–9a] have also been proven as effective chiral ligands for asymmetric metal catalysis.

Since the discovery of ferrocene in 1951,^[10] the cyclopentadienyl anion (Cp) has become a dominant class of ancillary ligands for a broad spectrum of metals.^[11–16] The 6π -electrons aromatic Cp is a good σ - and π -donor ligand and

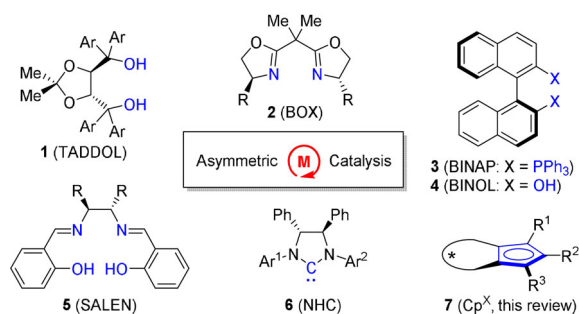


Figure 1. Selected privileged chiral ligands for asymmetric metal catalysis.

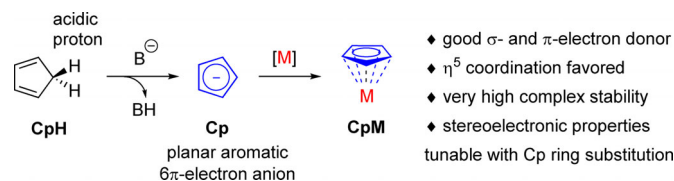
From the Contents

1. Introduction	3
2. Chiral Cyclopentadienyl Ligands	4
3. The Metal Complexes	8
4. Applications in Asymmetric Catalysis	10
5. Summary and Outlook	25

generally binds to a transition metal in the η^5 hapticity (Scheme 1), providing a remarkably high stability of the Cp metal complexes (CpM).^[15,16] This enables chemical transformations to occur at the metal center without affecting

the cyclopentadienyl moiety. In contrast, a higher risk of ring slippage is encountered with extended aromatic systems, such as indenyls, where η^3 coordination modes are more favored.^[17] Of particular importance in catalysis, the stereoelectronic properties of the metal center can be modified on demand by variation of the substituents on the cyclopentadienyl.^[18–21] For instance, replacing the hydrogen atoms for methyl groups on the Cp ring, commonly described as Cp^* , increases its σ -donating ability, which results in a higher ligand–metal dissociation energy.^[22,23] In addition, the facile rotation around the Cp–metal axis can be restricted by the presence of sterically demanding substituents on the Cp ring, providing additional conformational rigidity to the metal complex.^[24]

Distinct chiral complexes of d- and f-block metals bearing the cyclopentadienyl ligand have been shown to be efficient catalysts in a plethora of enantioselective reactions (Figure 2).



Scheme 1. General properties of the Cp ligand and its metal complexes.

[*] Dr. J. Mas-Roselló, Dr. A. G. Herrera,^[†] B. Audic,^[†] A. Laverny, Prof. Dr. N. Cramer
Laboratory of Asymmetric Catalysis and Synthesis
Institute of Chemical Sciences and Engineering
Ecole Polytechnique Fédérale de Lausanne (EPFL)
Lausanne (Switzerland)
E-mail: nicolai.cramer@epfl.ch

[†] These authors contributed equally to this work.

The ORCID identification number(s) for the author(s) of this article can be found under:
<https://doi.org/10.1002/anie.202008166>.



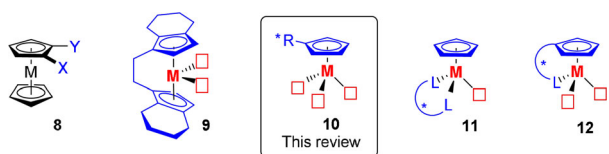


Figure 2. Chiral metal complexes bearing the Cp ligand and their available coordination sites.

Depending on the transformation, a minimum number of available coordination sites at the metal center is required to bind substrates and reactants for catalyst turnover. Some planar chiral metallocenes (**8**) are coordinatively saturated, serving as chemically inert backbones of heteroatom-coordinating ligands.^[25] For example, ferrocenyl diphosphine ligands, such as Josiphos, fall into this class.^[26] Other metallocenes, commonly known as *ansa*-metallocenes, offer two binding sites for catalysis (**9**).^[27] However, the previous designs are incompatible with transformations demanding 3 or more coordination sites.

This Review focuses on metal complexes bearing one single stabilizing Cp ligand, often named “half sandwich” or

“piano stool” complexes, in which the chirality belongs exclusively to the Cp ligand (**10**). These complexes have been shown to be powerful catalysts for a myriad of synthetically attractive enantioselective reactions requiring 3 or more catalytic active sites.^[8] Complexes with additional chiral ligands, such as chelates (**11**)^[28–30] or tethered to the Cp unit (**12**),^[31,32] that reduce the number of available coordination sites at the metal center, are excluded. We begin by discussing the strategic principles behind the ligand design, and provide an overview of the different ligand families and their comparative synthesis. Then we describe different general methods for ligand metallation, and show the application of the resulting Cp^x metal complexes in diverse highly enantioselective transformations. Finally, we discuss some current limitations of the art, and suggest new directions for future research efforts.

2. Chiral Cyclopentadienyl Ligands

The idea of employing chiral cyclopentadienyls as ligands for asymmetric metal catalysis dates back to 1978. First



Josep Mas-Roselló graduated in Chemistry at the University of Valencia (Spain). He obtained his PhD in 2017 from the University of Bristol (UK) under the supervision of Prof. J. Clayden. His research focused on the organo-alkali metal base-promoted C-functionalization of α -amino acids, working in collaboration with Syngenta Agrochemicals. He is currently a postdoctoral researcher in the group of Prof. N. Cramer, where he develops cyclopentadienyl metal complexes for asymmetric catalysis.



Aragorn Laverny received both an engineering degree in Organic Chemistry and a Master degree in biomolecules from the National graduate School of Montpellier (ENSCM) in France. During his master courses, he worked on stereoselective carbosulfenylation of alkenes under the supervision of Prof. Scott E. Denmark at UIUC. He started his PhD in the group of Prof. N. Cramer in November 2018, where he is currently working on cyclopentadienyl metal complexation.



Ana García Herraiz studied chemistry at the Complutense University of Madrid. Her Bachelor thesis in artificial metalloenzymes was performed in the group of Prof. G. Roelfes at the University of Groningen. For her MSc in Chemistry, she worked on copper catalysis in the group of Prof. B. Feringa. After an internship at Eli Lilly, she joined the group of Prof. M. G. Suero at ICIQ and obtained her PhD degree in 2019 for work on photoredox catalysis. She is currently a postdoctoral researcher in the group of Prof. N. Cramer.



Nicolai Cramer earned his PhD in 2005 at the University of Stuttgart under the guidance of Sabine Laschat. After a postdoctoral stint with Barry Trost at Stanford, he completed his habilitation at ETH Zurich from 2007 to 2010 with Erick Carreira. Subsequently, he moved to EPFL as assistant professor, was tenured in 2013 and promoted to full professor in 2015. His research encompasses sustainable enantioselective metal-catalyzed transformations and their implementation in synthesis. A focus is placed on asymmetric C–H functionalizations enabled by novel ligand designs.



Benoît Audic studied chemistry at the Université de Nantes. He performed an apprenticeship at Sanofi-Aventis to complete his undergraduate degree. During his Master's thesis at BASF he worked on the development of new insecticides. In October 2016, he started his PhD in the group of Prof. N. Cramer, where he works on chiral cyclopentadiene chemistry.

Krüger and co-workers reported the synthesis of (–)-menthol-derived cyclopentadiene **13** (Figure 3)^[33] and its metalation to different titanium and zirconium complexes.^[34] Most of the early examples were likewise built upon chiral natural sources. For example, Vollhardt started from (+)-tartaric acid or (+)-camphor in the syntheses of cyclopentadienes **14**^[35] and **15**,^[36] respectively. An exception was provided by Halterman, who, prompted by the success of related P, O, and N-based ligands containing the atropisomeric binaphthyl backbone, prepared the ligand precursor **16**.^[37]

However, none of these scaffolds were able to provide high levels of enantiocontrol in catalysis.^[6,34] After two decades of lethargy, a revised approach focusing on the design of the chiral cyclopentadienyl ligands has unlocked their potential in asymmetric synthesis.

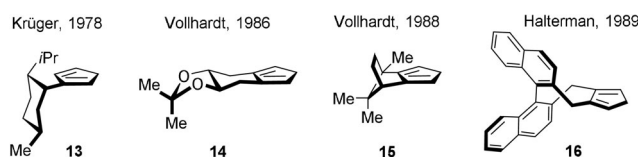
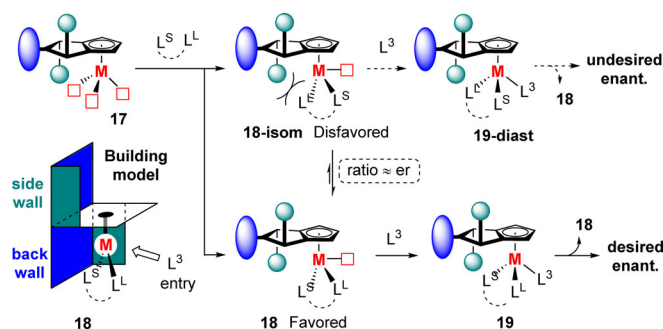


Figure 3. Selected first examples of chiral cyclopentadienes.

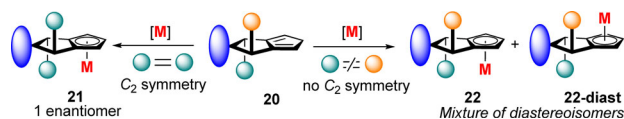
2.1. Ligand Design

In 2012, the group of Cramer envisaged a new Cp^X ligand architecture, comprised of two equal substituents on the flanks of the ligand backbone (green balls, sidewalls), and a large substituent at the rear (blue oval, backwall) (**17**).^[38] Those features were considered key to achieving high enantiocontrol by two proposed coordination requirements at the metal center (Scheme 2): Firstly, a strong preference for the tricoordinated species **18** over the alternative **18-isom**, governed by the stereoelectronic repulsion between the sidewall substituent proximal to the metal center and the large vs. small ligand (L^L or L^S, respectively). Secondly, control of the trajectory of the incoming third ligand (L³) with the facial shield provided by the ligand backwall, forming pseudotetrahedral complex **19** having a stereogenic metal center. The configuration of this intermediate would translate with high fidelity onto the formation of a single product enantiomer. The opposite configuration at the metal (**19-dia**) would form the other enantiomer.



Scheme 2. Proposed stereochemical modus operandi of Cp^X metal complexes.

Other important structural features of the Cp^X ligands were taken into consideration (Scheme 3). Ideally the cyclopentadiene pre-ligand **20** should be C₂ symmetric, with both faces of the Cp ring being equivalent, leading to a single enantiomeric ligand–metal complex **21** upon metallation. Otherwise, the separation of diastereomeric metal complexes (**22** and **22-dia**) could be tedious because they are often sensitive to chromatography at ambient conditions.



Scheme 3. Simpler Cp^X ligand metalation with C₂-symmetric scaffolds.

In addition, the scaffold should be easily sterically and electronically modifiable, preferably at a late stage of the synthesis, facilitating a rapid adaptation to the reactivity and selectivity requirements of the target transformation. All these ligand design principles were followed by the group of Cramer who, developing on Cp^X predecessors **14** and **16**, reported the synthesis of two new mannitol-^[38] and BINOL-derived^[39] scaffolds (Figure 4). Their successful application in enantioselective Rh-catalysis (Section 4.2) validated the authors' proposal, setting the basis for future ligand classes.

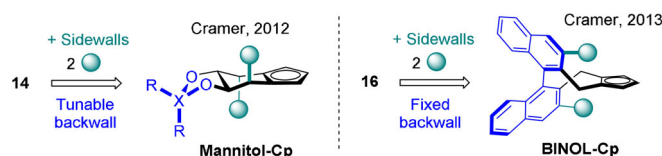


Figure 4. Improved Cp^X ligands based on novel design principles.

2.2. Overview of the Existing Ligand Families

Several different chiral cyclopentadienyl ligands have been developed over the last decade. They can be grouped into six different classes based on their structural footprint (Figure 5). For each family, we detail: i) the publication year of the first developed ligand and the corresponding author(s); ii) an interval of synthetic steps to access all members; iii) the approximate extension of the family; iv) the number of disclosed applications in metal-catalyzed enantioselective transformations, and the metal elements employed. Further, the main synthetic routes towards the chiral cyclopentadiene ligand precursors are discussed in Section 2.3.

The oldest selected ligand class is **Mannitol-Cp**, first reported by Cramer and co-workers in 2012.^[38] Its characteristic cyclohexane-fused ring presents two modifiable points: the 1,2-diol functionality, often protected as an acetal, and the substituents (R²) at the carbon atom in α position to the Cp. A total of seven derivatives are known for this family, enjoying application in two different Rh-catalyzed enantioselective transformations, despite its low molecular weight and average modularity. The same year, the groups of Ward and Rovis



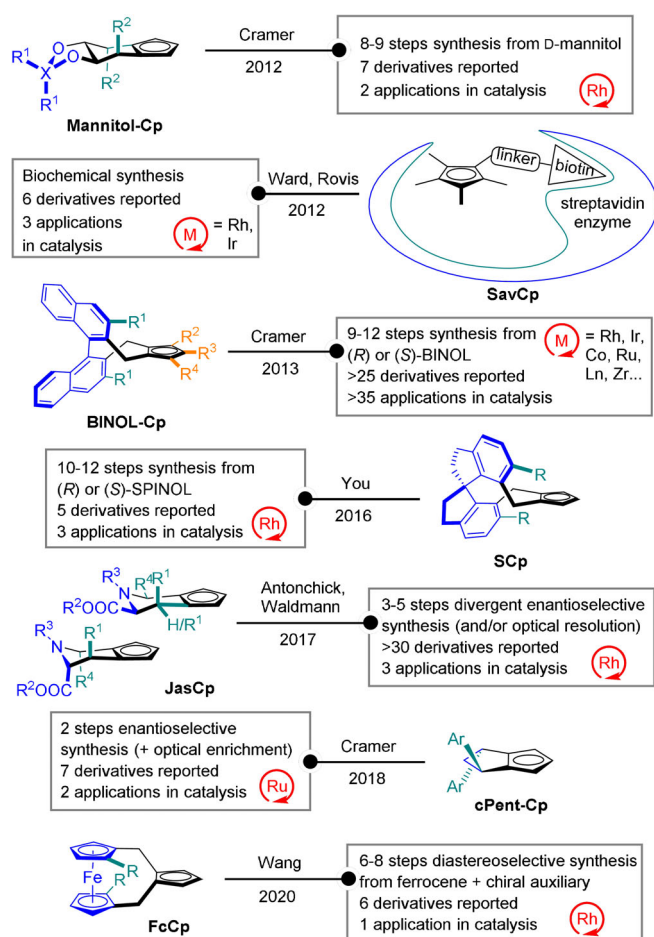


Figure 5. An overview of the current families of Cp^{X} ligands.

collaboratively introduced a macromolecular streptavidin-enzyme-linked Cp ligand, **SavCp**, and its application in Rh-catalysis.^[40] In principle, the possibility of performing an unlimited number of protein mutations should facilitate the “directed evolution” of the ligand towards a specific transformation. However, in practice, the need for mutagenesis techniques and the higher sensitivity of enzymes to harsh experimental conditions (e.g. temperature, solvent, pH) may explain why this ligand family has found limited applications.

The C_2 -symmetric atropochiral **BINOL-Cp** scaffold, first disclosed by Cramer in 2013,^[39] represents by far the most widely applied ligand class, finding success in over 35 different enantioselective transformations as complexes of transition metals (Rh, Ru, Ir, Co) as well as rare-earth metals (Sc, Y, La, Sm, Gd, etc.). The key structural feature responsible for its broad success is the introduction of sterically and electronically tunable *ortho*-substituents (sidewalls, R^1) on a fixed binaphthyl backbone (backwall). Moreover, recent studies demonstrated that additional substitution at the Cp ring (R^2 , R^3 , R^4) can significantly change the complexes’ reactivity and selectivity.^[41,42] Over 25 derivatives are known for this class, with constant efforts towards shorter, more efficient syntheses being made.^[43,44] In 2016, You and co-workers presented a second axially chiral C_2 -symmetric ligand family, named **SCp** because of its spirocyclic backbone.^[45] Being similar in

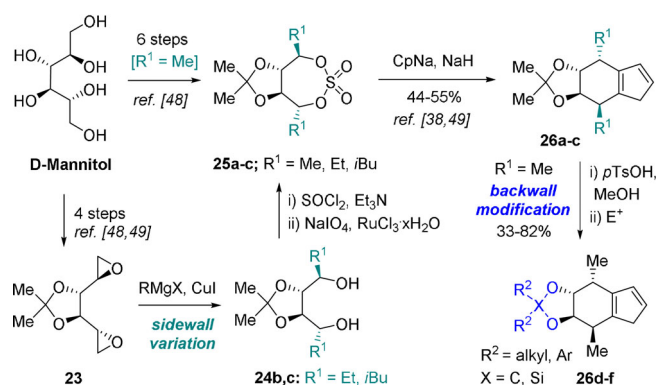
design to the **BINOL-Cp** predecessor, a comparative x-ray crystal structure analysis of their $\text{Cp}^{\text{X}}\text{Rh}(\text{C}_2\text{H}_4)_2$ complexes indicated that the R substituents in **SCp** were closer in space to the metal center than the R^1 substituents of **BINOL-Cp** in the solid state. This could translate into a better stereocontrol at the metal center provided by the **SCp** ligand. However, various direct ligand comparisons in different Rh-catalyzed transformations showed complementary behavior between the two complexes (section 4.2).

In 2017, Antonchick and Waldmann reported a novel class of piperidine-fused **JasCp** ligands with four adjustable positions.^[46] On the one hand, the straightforward synthesis of the diene precursors, by means of enantioselective catalysis, allowed the construction of over 30 derivatives in a short time frame. On the other hand, the need to upgrade the enantiomeric excess of the ligands and their absence of C_2 symmetry mean additional efforts and complications for their use as metal complexes in catalysis. So far, exclusively the inventors have applied them to three novel Rh-catalyzed enantioselective transformations. More recently, the Cramer group developed another class of low-molecular-weight Cp^{X} ligands, **cPent-Cp**, bearing two electronically and sterically tunable aryl substituents at their cyclopentane-fused ring.^[47a] The convenient two-step enantioselective synthesis of the C_2 -symmetric cPent-CpH pre-ligands, as nearly single enantiomers, may attract further research into this young family. Their potential has been demonstrated in two Ru^{II} -catalyzed transformations (Section 4.4) where they outperformed existing **BINOL-Cp** ligands. Notably, other metal complexes such as $\text{Cp}^{\text{X}}\text{Co}^{\text{III}}$,^[58] $\text{Cp}^{\text{X}}\text{Rh}^{\text{I}}$, and $\text{Cp}^{\text{X}}\text{Ir}^{\text{I}}$ are known,^[47a] but their successful application in asymmetric catalysis is yet to be uncovered.

In 2020, Wang et al. introduced a novel C_2 -symmetric ligand class (**FcCp**) equipped with a planar chiral ferrocene backbone bearing identical modifiable 2,2'-substituents (R) and 1,1'-dimethylene links to the free Cp ring.^[47b] Six different analogs were accessed in 6–8 steps from ferrocene by using an amine chiral auxiliary, and their corresponding Rh^{I} , Ir^{I} , and Ru^{II} complexes were reported. X-ray crystal structure analysis indicated that, in the solid state, the chiral ferrocenyl moiety is positioned away from the metal center. The authors tested the Rh^{I} complexes in one catalytic transformation with excellent reactivity (>99% yield) and moderate enantioselectivity (67% *ee*) for a model substrate. Noteworthy, related complexes bearing a **BINOL-Cp** ligand provided enhanced enantioselectivity (70% *ee*) but lower reactivity (50% yield). Further studies are needed to prove the power and utility of **FcCp** ligands in enantioselective catalysis.

2.3. Syntheses of $\text{Cp}^{\text{X}}\text{H}$ Diene Pre-Ligands

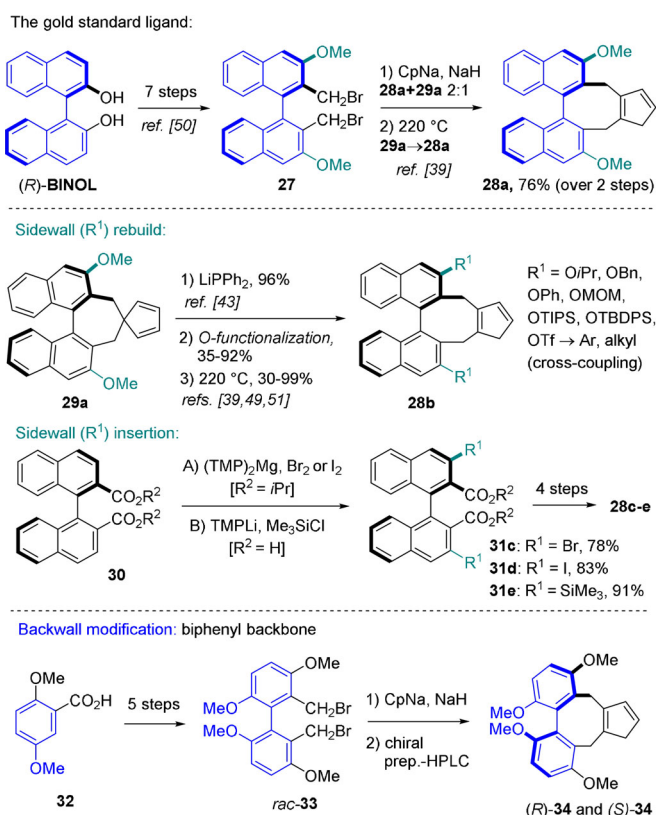
The syntheses of **Mannitol-CpH** dienes **26**^[38,48,49] start from natural D-mannitol and follow two alternative routes to access different alkyl-substituted (R^1 , sidewall) derivatives of the common cyclic sulfate intermediate **25** (Scheme 4). Subsequent dialkylation with sodium cyclopentadienide afforded dienes **26a–c** bearing an acetonide-derived back-wall. Further, a two-step sequence of ketal cleavage–diol



Scheme 4. Cramer's synthesis of D-mannitol-derived cyclopentadienes.

functionalization allowed the introduction of sterically different ketals and cyclic silylethers as ligand backwall (**26d-f**).

Concerning the **BINOL-Cp** family, the synthesis of diene **28a**, arguably its most widely used member, starts from 1,1'-bi(2-naphthol) **BINOL** equally accessible in the *R*- or *S*-enantiomeric form (Scheme 5). A 7-step protocol delivered dibromide **27** bearing *ortho*-methoxy substituents.^[50] Subsequent standard dialkylation with sodium cyclopentadienide afforded a 2:1 mixture of 1,2-disubstituted cyclopentadiene **28a** and spirocyclic diene **29a**, respectively.^[39] The mixture could be either separated by trituration in ethyl acetate or converted into **28a** upon heating in high overall yield. Noteworthy, **28a** and substituted cyclopentadienes in general



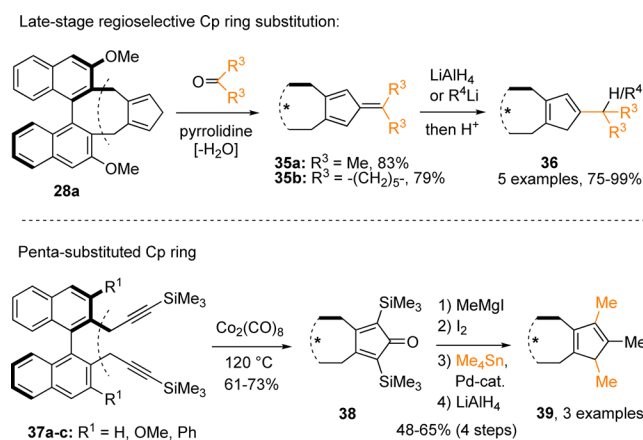
Scheme 5. Synthesis of Cramer's atropochiral biaryl $\text{Cp}^{\text{X}}\text{H}$ dienes.

are often isolated as inconsequential mixtures of double-bond isomers, converging to a single ligand–metal complex upon metalation (see below); we chose to depict them as one isomer for clarity. From **29a**, a 3-step sequence of demethylation,^[43] O-functionalization, and thermal rearrangement allowed the late-stage sidewall variation (R^1). Accordingly, $\text{Cp}^{\text{X}}\text{H}$ pre-ligands **28b** having a variety of ethers, alkyl and aryl substituents^[39,49,51] were accessed. In addition, dienes **28c-e** bearing halide or silyl functionalities were recently made via *ortho*-metalation/electrophilic quenching of diester **30**.^[44] Altogether, a broad range of stereoelectronic modulations of the sidewalls are available. In the same report, a modification of the naphthyl backwall by a simpler atropochiral biphenyl backbone was disclosed. Starting from achiral carboxylic acid **32**, both the *R*- and *S*-enantiomers of cyclopentadiene **34** were prepared in 7 steps ending with a nonideal chiral resolution of *rac*-**34** by preparative HPLC.

Bulkier analogs of pre-ligands **28** can result from additional substitution at the Cp ring. For example, a range of trialkyl trisubstituted cyclopentadienes **36** were prepared by the Cramer group from **28a** via a 2-step sequence (Scheme 6):^[41] first, condensation with a ketone, forming the corresponding fulvenes **35**, then hydride or organolithium addition to the double bond. Recently, You and co-workers reported the synthesis of Cp pentaalkyl analogs **39** from dialkynes **37** through a key cobalt-promoted carbonylative cyclization, followed by multistep functionalization of the resulting dienone intermediates **38**.^[42]

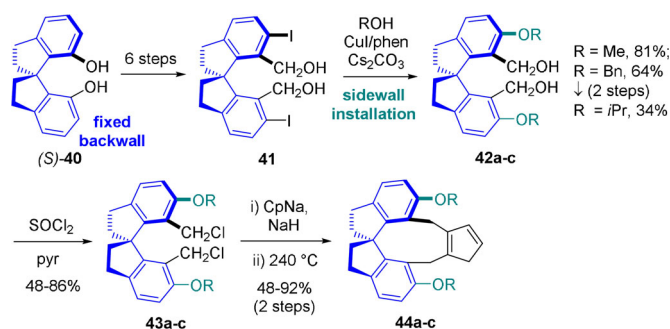
The synthetic route to SCpH pre-ligands **44** (Scheme 7), containing a fixed 1,1-spirobiindane skeleton, is strategically similar to the previous one from **BINOL** to **28a**. The more expensive **SPINOL** starting material **40** was converted into the diaryl diiodide **41** in 6 linear steps.^[45,52] From here, dienes **44a-c** were synthesized via a key Ullmann coupling, enabling the middle-stage insertion of sterically different alkoxy *ortho*-substituents as the ligand sidewall.

The previously described chiral cyclopentadiene syntheses rely on the chiral pool strategy, starting from an enantiopure molecule which then undergoes a series of functional group manipulations. More recent approaches employ asymmetric catalysis to construct the $\text{Cp}^{\text{X}}\text{H}$ pre-



Scheme 6. Synthesis of BINOL-derived tri- and pentasubstituted $\text{Cp}^{\text{X}}\text{H}$ dienes.

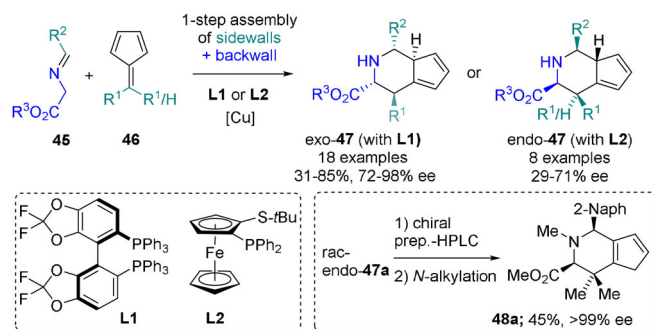




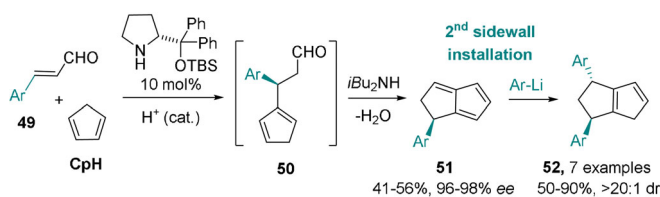
Scheme 7. You's synthesis of SPINOL-derived SCpH chiral dienes.

ligand from achiral simple building blocks. While those facilitate a faster build-up of molecular complexity, an excellent stereocontrol in the enantioselective step is desirable in order to avoid extra efforts to upgrade the optical purity of the products. For example, Waldmann et al. reported a copper-catalyzed enantioselective [6+3] cycloaddition of imino esters **45** with fulvenes **46** as the key step towards JasCp dienes **3** (Scheme 8).^[46] Chiral phosphine ligands **L1** or **L2** provided excellent diastereoselectivity for the *exo*- or *endo*-products **47**, respectively, enabling a rapid pre-ligand library creation. However, given the average moderate to high enantioselectivities obtained, optical enrichment of **47** is required for their useful application in enantioselective catalysis. In fact, for some analogs their synthesis as racemates followed by optical resolution via chiral preparative HPLC may be more convenient, as reported by the authors for best-in-class **48a**, the *N*-methyl derivative of **47a**.

Lastly, cyclopentane-fused diaryl pre-ligands **52** were accessed by the group of Cramer in 2 steps from CpH and cinnamaldehydes **49** (Scheme 9). The initial key enantioselective step involved a tandem organo-catalyzed ene-type reaction–intramolecular condensation of intermediate **50**,^[53]



Scheme 8. Antonchick and Waldmann's synthesis of JasCpH pre-ligands.



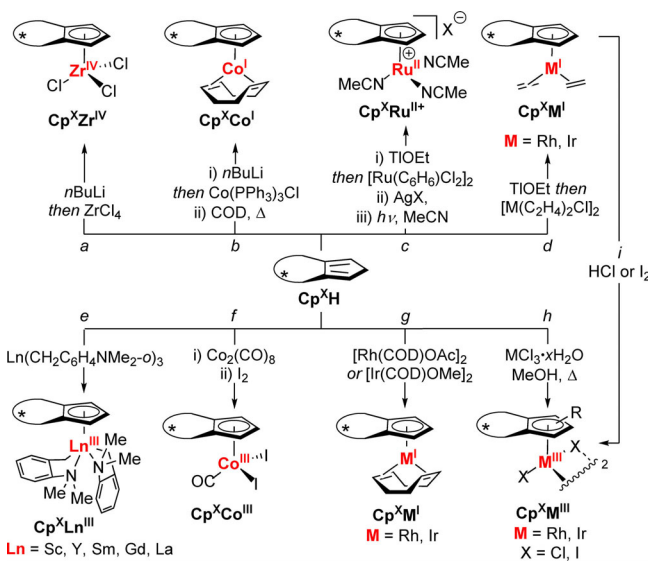
Scheme 9. Cramer's synthesis of diaryl-cyclopentane-fused chiral dienes.

delivering chiral cyclopentane-fused fulvenes **51** in excellent enantioselectivity and moderate yields.^[47a] Subsequent addition of aryl lithium compounds across the fulvenes yielded *C*₂-symmetric cyclopentadienes **52** as single diastereoisomers with overall 98:2–99:1 enantiomeric ratio, qualifying to be used directly in catalysis without the need for additional optical enrichment.

3. The Metal Complexes

Along with the development of the ligand families, complexation methods are required to access the appropriate metal catalysts. Importantly, the reaction conditions must tolerate the different ligand functional groups and stabilities. Frequently, long complexation times, the generation of incompatible byproducts, or solvents make in situ complexation of the Cp^XH dienes and their direct use in catalysis impossible, unlike other privileged ligands (phosphines, BOX, etc.). Often, Cp^X metal complexes are pre-formed and purified prior to catalysis. The different existing synthetic strategies towards pre-catalysts depend on the metal, its oxidation state, the nature of the additional stabilizing ligands, and the substitution of the Cp ring.

Two main synthetic strategies are used involving either ligand transmetalation (Scheme 10, methods a–d) or direct metalation (Scheme 10, methods e–h). The former relies on the deprotonation of Cp^XH by organolithium or thallium salts, followed by metal substitution with an appropriate halogenated complex; whereas complexes of base metals [Cp^XZr^{IV},^[54] Cp^XCo^I^[55]] are typically accessed via Li-Cp^X (methods a and b), noble metals [Cp^XRu^{II},^[51] Cp^XRh^I,^[38,39] Cp^XIr^{III}^[56]] are more effectively transmetalated with thallium (methods c and d). In the case of ruthenium (method c), this strategy enables the isolation of cationic sandwich complexes [Cp^XRu(C₆H₆)⁺]Cl[−] while preventing the formation of ruthenocene, (Cp^X)₂Ru. From the former, chloride anion

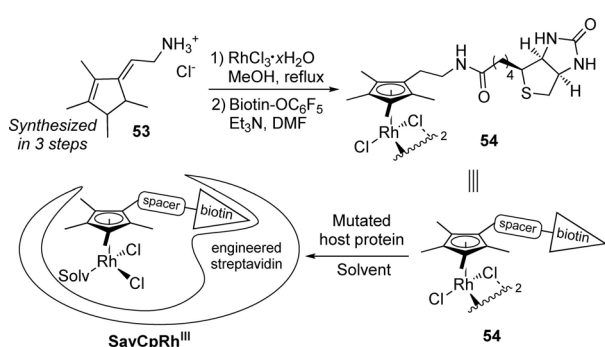


Scheme 10. Cp^XH pre-ligand complexation via transmetalation (a–d) or direct metalation (e–h).

exchange and benzene decomplexation by photolysis in acetonitrile affords catalytically active $\text{Cp}^X\text{Ru}^{\text{II}}$ complexes.

In contrast, rare-earth metal pre-catalysts $\text{Cp}^X\text{Ln}^{\text{III}}$ are readily synthesized via direct acid–base ligand exchange between Cp^XH and the corresponding tris(aminobenzyl) metal complex^[57] (method e). $\text{Cp}^X\text{Co}^{\text{III}}$ complexes are accessed from Cp^XH by reaction with $\text{Co}_2(\text{CO})_8$ to deliver $\text{Cp}^X\text{Co}^{\text{I}}(\text{CO})_2$, followed by in situ oxidation with I_2 ^[58] (method f). Various approaches exist to access $\text{Cp}^X\text{Rh}^{\text{I}}$ and $\text{Cp}^X\text{Ir}^{\text{I}}$ complexes bearing different bis-alkene stabilizing ligands (methods d and g). Comparatively, the chelating 1,5-cyclooctadiene (COD) ligand provides higher stability to the complexes than diethylene, facilitating their synthesis and isolation. While diethylene complexes are accessed from Cp^XH via two-step metalation to thallium (Cp^XTl transmetalation with the corresponding $[\text{M}(\text{C}_2\text{H}_4)_2\text{Cl}]_2$ source; method d), a more convenient approach involves the direct complexation of Cp^XH to an acetoxy- or alkoxy-metal complex bearing a COD ligand by deprotonation/anionic ligand exchange (method g).^[59] The mild reaction conditions employed by this variant allow the resulting metal complexes to be directly engaged in catalysis. $\text{Cp}^X\text{Rh}^{\text{III}}$ and $\text{Cp}^X\text{Ir}^{\text{III}}$ dimeric halide complexes are commonly accessed in two different ways depending on the substitution of Cp^XH . Generally, heavily substituted Cp units, such as Cp^* , are more stable to harsh reaction conditions. Whereas tri- and pentasubstituted Cp^XH can be directly metalated with RhCl_3 or IrCl_3 hydrates upon heating (method h),^[42,60] disubstituted $\text{Cp}^X\text{M}^{\text{III}}$ derivatives are accessed by oxidation of their $\text{Cp}^X\text{M}^{\text{I}}$ precursors with HCl or iodine (method i).^[41,61,62] The former method was employed in the synthesis of metalloenzyme **SavCpRh^{III}** (Scheme 11).

Starting from Cp^* tautomer **53**, the biotin-linked $\text{Cp}^X\text{Rh}^{\text{III}}$ dichloride dimer **54** was accessed in two steps via direct metalation with RhCl_3 ,^[63] followed by amide coupling.^[40] Then, **54** was associated to a range of streptavidin enzyme mutants to create a macromolecular chiral environment around the metal center.



Scheme 11. Synthesis of biotinylated $\text{Cp}^X\text{Rh}^{\text{III}}$ metalloenzymes.

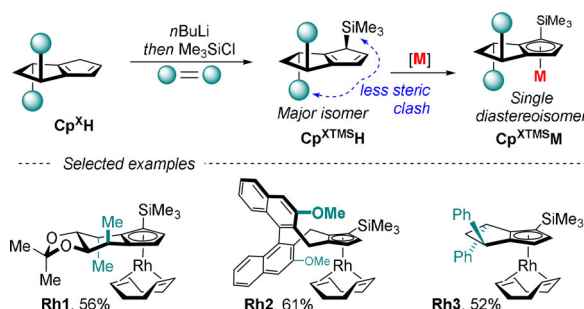
3.1. Facial Selectivity and Planar Chirality

To avoid complex facial diastereoselective Cp^XH diene metalation, most ligand families are designed with C_2 symmetry (see Scheme 3). An exception was found in the

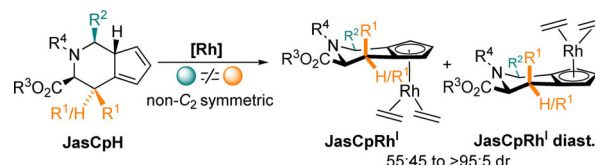
case of Cp^{XTMS} derivatives (Scheme 12).^[59] Although the introduction of a trimethylsilyl group on the Cp^XH ring breaks the ligand's C_2 symmetry, one major diastereoisomer is favored ($\text{Cp}^{\text{XTMS}}\text{H}$) in order to minimize steric repulsion between the $-\text{SiMe}_3$ group and the ligand sidewall substituents. Subsequent deprotonation/metalation proceeds with excellent facial selectivity, as observed, for example, in the complexation of three different Cp^{XTMS} derivatives (**Rh1–3**) to rhodium(I).

In contrast, **JasCpH** pre-ligands typically present issues of facial-selective metalation (Scheme 13). In most of the analogs, the different substituents do not provide significant steric bias for the metal to choose between one of the two distinct faces of the ligand. Thus, their metalation to rhodium often leads to a mixture of **JasCpRh^I** diastereoisomers, which are separated under elaborate chromatographic conditions (-40°C , argon pressure), or sometimes inseparable.^[46]

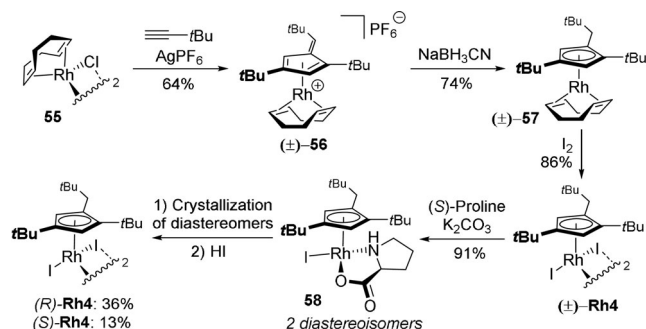
The Perekalin group adopted a different synthetic approach towards chiral Cp^XRh complexes, which relied exclusively on planar chirality (Scheme 14).^[64] Starting from $[\text{Rh}(\text{COD})\text{Cl}]_2$ (**55**), a metal-mediated $[2+2+1]$ cyclotrimerization of *tert*-butylacetylene generated a cationic fulvene Rh



Scheme 12. High facial selectivity in the metalation of $\text{Cp}^{\text{XTMS}}\text{H}$; selected examples.



Scheme 13. Facial-selectivity issues in the metalation of **JasCpH**.

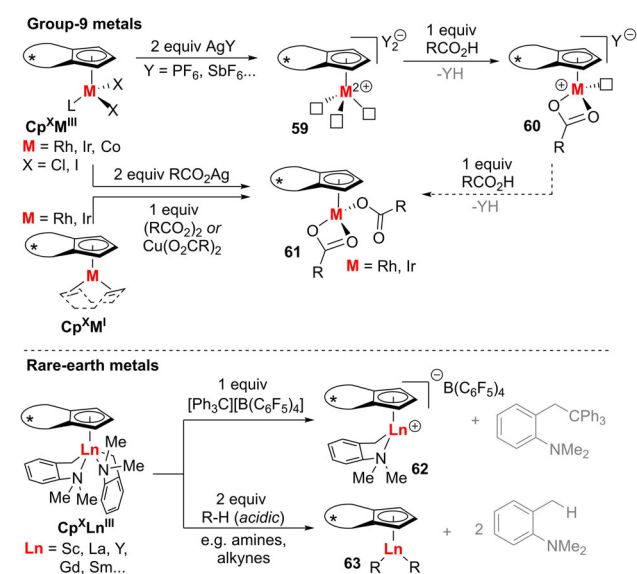


Scheme 14. Perekalin's synthesis of a planar chiral $\text{Cp}^X\text{Rh}^{\text{III}}$ complex.

complex (\pm)-**56**. Then, hydride addition across the fulvene double bond, followed by Rh oxidation with iodine, delivered $\text{Cp}^{\text{X}}\text{Rh}^{\text{III}}$ iodide dimer (\pm)-**Rh4** in high overall yield. The racemic mixture was resolved after a 3-step sequence of iodide/(*S*)-proline ligand exchange, diastereomeric crystallization of **58**, and proline removal in acidic media (HI). Overall, both enantiomers of planar chiral $\text{Cp}^{\text{X}}\text{Rh}^{\text{III}}$ complex **Rh4** were rapidly accessed. However, the structural variation of the Cp ligand was limited to bulky alkyl substituents by the initial alkyne cyclotrimerization step. Perhaps a stereoselective complexation of a preformed prochiral $\text{Cp}^{\text{X}}\text{H}$ diene would enhance the modularity and practicality of this methodology, avoiding tedious chiral resolution techniques.

3.2. Pre-Catalyst Activation

The formation of the active catalyst is a key process in catalysis and has direct implications in the reaction efficiency. Generally, group-9 $\text{Cp}^{\text{X}}\text{M}^{\text{III}}$ halide complexes ($\text{M} = \text{Co}, \text{Rh}, \text{Ir}$) are activated in situ by halide abstraction with non-coordinating silver salts (Scheme 15), forming dicationic complexes **59** with three free coordination sites for substrate binding and catalyst turnover. In transformations involving C–H bond activation via a carboxylate-assisted CMD mechanism (Sections 4.2, 4.3, and 4.5), complexes **60** or **61** are required. Those can be accessed in different ways. From dicationic **59**, an equimolar amount of acid yields monocationic species **60**, or neutral **61** with two acid equivalents. Alternatively, **61** can be formed directly from $\text{Cp}^{\text{X}}\text{M}^{\text{III}}$ by halide abstraction with a silver carboxylate salt. More conveniently, these active catalysts can be generated from low-valent $\text{Cp}^{\text{X}}\text{M}^{\text{I}}$ pre-catalysts after in situ oxidation with peroxides^[38] or copper salts,^[65a] avoiding the use of costly silver salts. Compared to $\text{Cp}^{\text{X}}\text{M}^{\text{I}}$ -diethylene complexes, analogs bearing a more stabilizing COD ligand require heating or stronger oxidants for activation. Rare-earth metal catalysts **62**



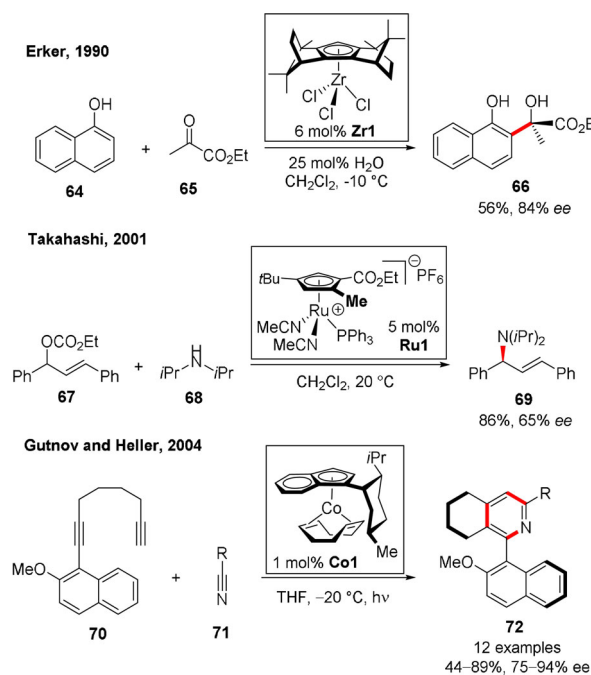
Scheme 15. General methods for in situ pre-catalyst activation.

and **63** are generated by acid–base ligand exchange from bis(aminobenzyl) pre-catalysts $\text{Cp}^{\text{X}}\text{Ln}^{\text{III}}$ (see Section 4.6 for applications). A reaction with equimolar amounts of $[\text{Ph}_3\text{C}][\text{B}(\text{C}_6\text{F}_5)_4]$ forms cationic complex **62**, which allows metal coordination to aprotic directing groups such as pyridines.^[57] Alternatively, protic substrates (e.g. terminal alkynes, secondary amines) undergo direct ligand exchange to yield the active catalysts **63**.^[66,67]

4. Applications in Asymmetric Catalysis

4.1. Early Work

Before the soar development of versatile chiral Cp^{X} metal complexes for asymmetric catalysis, three highly enantioselective transformations were reported showing limited catalyst modularity and reaction scope (Scheme 16). In 1990, Erker and co-workers described the hydroxyalkylation of 1-naphthol (**64**) with ethyl pyruvate (**65**) catalyzed by (+)-camphor-derived $\text{Cp}^{\text{X}}\text{Zr}^{\text{IV}}$ complex **Zr1**.^[54] In this Friedel–Crafts-type reaction, the chiral catalyst is believed to act as a Lewis acid. A decade later, Takahashi et al. reported the first enantioselective amine allylation powered by a planar chiral $\text{Cp}^{\text{X}}\text{Ru}^{\text{II}}$ complex **Ru1**.^[31] Analogous catalysts with the phosphine ligand anchored to the Cp ring delivered higher reactivity and enantioselectivity, however those fall outside the scope of this Review. In 2004, Gutnov and Heller employed the (–)-menthol-derived $\text{Cp}^{\text{X}}\text{Co}^{\text{I}}$ complex **Co1** as catalyst in the cyclotrimerization of diyne **70** with nitriles **71**, providing axially chiral pyridines **72** in modest to good yields and with high enantioselectivities.^[55a] Additional indenyl-based chiral Co^{I} complexes were later evaluated,^[55b] and the



Scheme 16. First highly enantioselective applications of chiral Cp^{X} metal complexes.

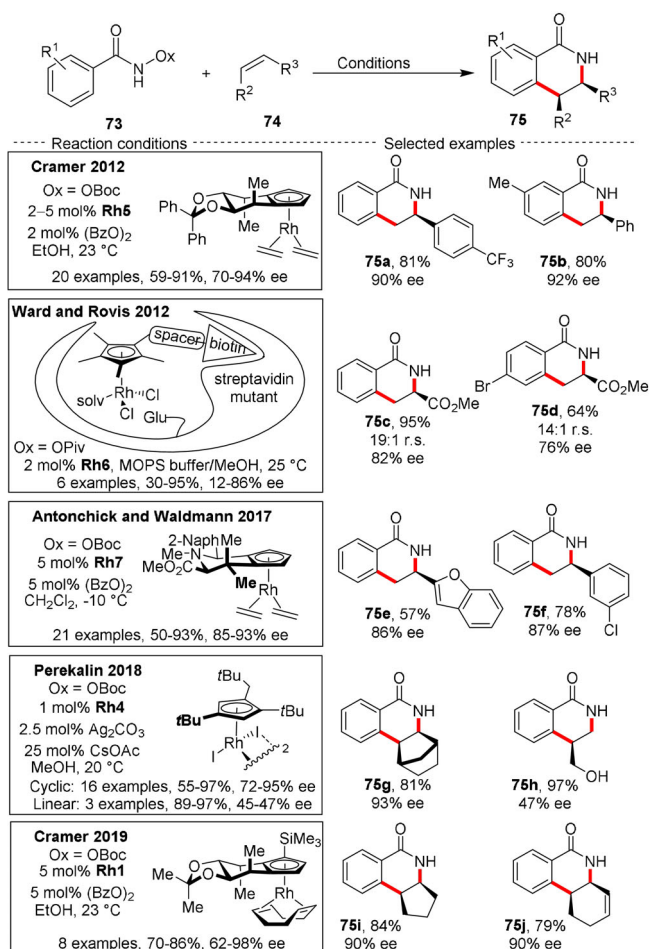
protocol was extended to the [2+2+2] cyclotrimerization of propargylic phosphine oxides with two acetylene units.^[68] These three methodologies represent an early proof of concept in the field of Cp^X metal catalysis.

4.2. Rh^{III} Catalysis

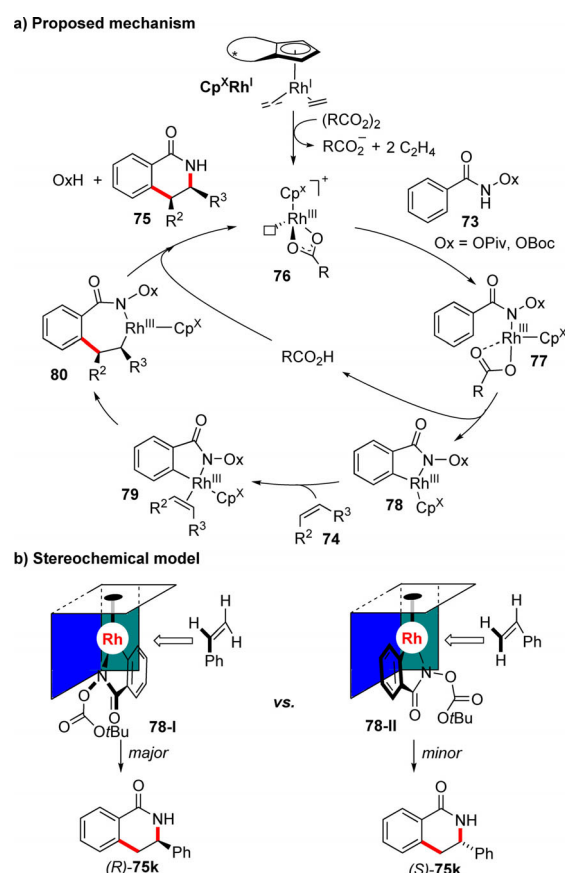
At the beginning of the last decade, the attractiveness of metal-catalyzed C–H functionalization chemistry aided the rapid development of Cp^X ligands.^[8] In 2012, the Cramer^[38] and Rovis^[40] groups independently reported two enantioselective syntheses of dihydroisoquinolinones **75** via Rh^{III}-catalyzed C–H activation of hydroxamates **73** and coupling with alkenes **74** (Scheme 17). In both methodologies, the formal [4+2] annulation reaction proceeded in high regioselectivity towards the product C3 isomer. Cramer and co-workers employed the **Rh5** complex containing a small-molecule Mannitol-Cp^X ligand, which performed better with styrene coupling partners. Complementarily, the SavCp metalloenzyme **Rh6** by Rovis and Ward was most efficient with acrylates. Compared to styrenes, smaller acrylates are best suited to approach the metal center in a confined chiral environment. Moreover, their electron-poor character

matches the more electron-rich pentaalkyl-substituted Cp ring of SavCp, compared to disubstituted Mannitol-Cp^X. Later this transformation served as a benchmark reaction for testing new Cp^XRh complexes. For example, **Rh7** bearing the JasCp ligand reached comparable levels of efficiency as **Rh5**, but at lower reaction temperature.^[46] The planar chiral complex **Rh4** showed its best results with strained alkenes, such as norbornenes, and provided the products **75** in high yields and enantioselectivities at lower catalyst loading (1 mol%).^[64] Interestingly, primary alkenes led to reversal of the regioselectivity, forming the C4-substituted isomer of the products (**75h**), however with moderate enantioselectivity. Finally, the use of Mannitol-Cp^{XTMS} **Rh1** allowed high enantioselectivities with non-strained cyclic alkenes, outperforming the parent derivative **Rh5**.^[59]

The generally accepted mechanism for the reaction is shown in Scheme 18a. After in situ generation of the active Cp^XRh^{III} catalyst **76**, the hydroxamate functionality coordinates to the metal center (**77**). Subsequently, a carboxylate-assisted concerted metalation–deprotonation (CMD) takes place,^[69] generating a 5-membered rhodacycle **78** and a molecule of carboxylic acid (RCO₂H). Then, an enantiodetermining migratory insertion into the alkene **74** leads to chiral-at-metal intermediate **80**, which undergoes tandem reductive elimination/oxidative cleavage of the N–O bond, forming the dihydroisoquinolone product **75** and regenerating the cata-



Scheme 17. Benchmark synthesis of dihydroisoquinolinones catalyzed by Cp^XRh^{III} complexes.

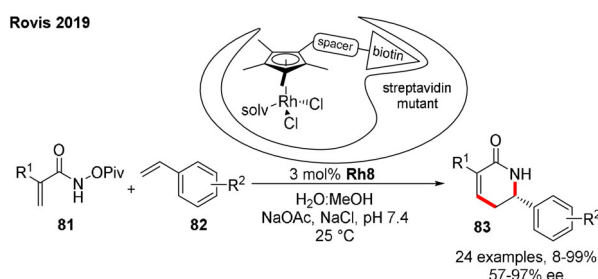


Scheme 18. Mechanism of the hydroxamate-directed Rh^{III}-catalyzed [4+2] annulation and stereochemical rationale.



lyst. Noteworthy, the hydroxamate functionality acts both as the directing group for C–H functionalization and as the internal oxidant (Ox). As in the general stereochemical model discussed in Scheme 2, the cyclometalation of **73** is controlled by the chiral environment provided by the Cp^X ligand, which favors one conformation of the tricoordinated species (**78-I**, Scheme 18b). Next the ligand backwall forces the approach of the olefin partner from the front side. The phenyl group aligns with the hydroxamate, leading to a diastereoselective coordination of the olefin to the metal center prior to the enantiodetermining migratory insertion step.

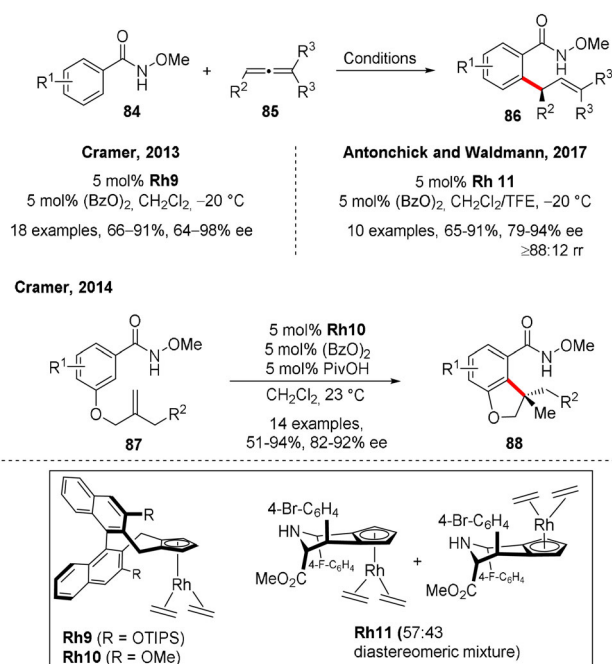
Recently, the Rovis group extended the scope of the hydroxamate coupling partner from benzamide to acrylamide derivatives **81** (Scheme 19).^[70] The reaction proceeds via alkene C–H activation and coupling with styrenes **82** resulting in the formation of dihydropyridones **83**. The steric and electronic variation of both alkene partners led to high disparity in the product yields (8–99%) and enantioselectivities (57–97% *ee*).



Scheme 19. Synthesis of dihydropyridones catalyzed by SavCpRh^{III} complexes.

Rhodium is by far the most employed transition metal in combination with Cp^X ligands.^[71] Besides the generation of enantioenriched δ -lactams via [4+2] annulation, Cp^XRh^{III} catalysts have been successful in a diverse set of mechanistically related transformations, giving access to a wide range of enantioenriched molecules. Those contain point, axial, and planar chirality, including the generation of heteroatom stereocenters. Whereas most of the transformations involve activation of aryl C–H bonds, few recent examples showed the functionalization of alkenyl C–H bonds. The most widely employed directing groups are hydroxamic acid derivatives, followed by hydroxy and pyridyl groups. Other functionalities, such as sulfonamides, ketoximes, nitrones, sulfonyl imines, amides, or phosphinic amides, have also been successful. Among the electrophilic coupling partner, diazo compounds, alkenes, and allenes have been found to be competent in the reactions.

In 2013, the Cramer group reported the intermolecular coupling of benzohydroxamates **84** with allenes **85** (Scheme 20).^[39] In this transformation, BINOL-CpRh complexes outperformed Mannitol-CpRh⁵. In particular, **Rh9** bearing the Cp^X ligand with bulky OTIPS *ortho*-substituents was optimal to provide good yields (66–91%) and high enantiocontrol (up to 98% *ee*) for the synthesis of allylated products **86**. Due to sterics, the reaction is selective toward the

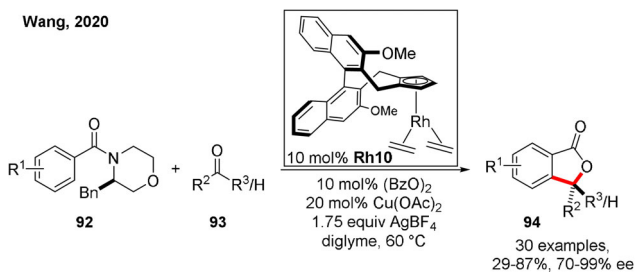
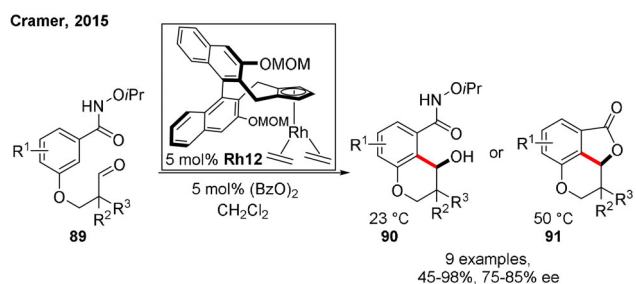


Scheme 20. Cp^XRh^{III}-catalyzed C–H bond functionalization of N-methoxybenzamides with allenes and internal alkenes.

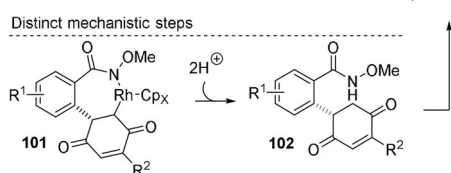
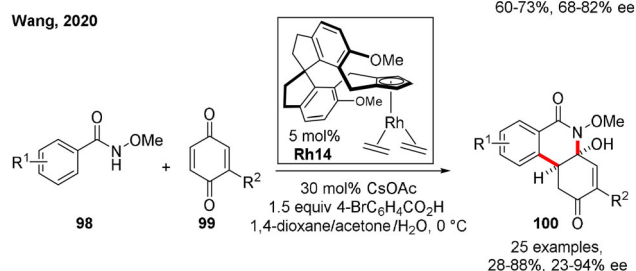
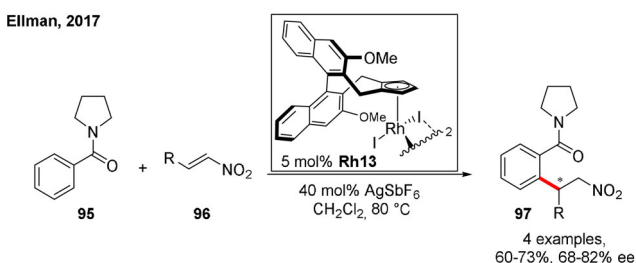
less substituted π bond of the allene. The use of a diastereomeric mixture of JasCp complexes **Rh11** showed similar levels of efficiency.^[46] The authors demonstrated that, conveniently in this case, both individual diastereoisomers provide similar reactivity and enantioselectivity. Later internal alkenes **87** were shown to engage in the reaction forming dihydrobenzofurans **88**.^[72] Good to excellent yields and high enantioselectivities were achieved with the complex BINOL-CpRh¹⁰. Noteworthy, the reversibility of the C–H activation step was key for reactivity. While metalation of the sterically more accessible *ortho* C–H bond was unproductive, a favorable 5-*exo-trig* cyclization reaction occurred between the other *ortho* C–H bond of the arene and the internal 1,1-allyl ether. After alkene migratory insertion, protodemetalation was favored over C–N bond coupling in the presence of catalytic amounts of pivalic acid, resulting in an increased yield of product **88**.

The intramolecular cyclization reaction was extended to aldehydes as π acceptor (Scheme 21).^[49] Whereas free alcohols **90** were selectively obtained at room temperature, heating of the reaction favored intramolecular cyclization to the corresponding lactones **91**. In 2020, Wang et al. developed an intermolecular version of this reaction using external carbonyl acceptors.^[73] Similarly, high reaction temperature favored the lactonization to 3-substituted phthalides **94**. Notably, the matching effect between a chiral tertiary amide directing group, acting as chiral auxiliary, and catalyst **Rh10** was crucial to reach high enantioselectivity. Nonideal stoichiometric amounts of an expensive silver salt were required to reach high yields.

Michael acceptors are also suitable coupling partners for the C–H functionalization of benzamide derivatives **95** (Scheme 22). In 2017, Ellman's group reported four enantioselective examples of conjugate addition to nitroalkenes **96**



Scheme 21. Cp^xRh^{III}-catalyzed benzamide C–H bond functionalization with internal and external aldehydes.

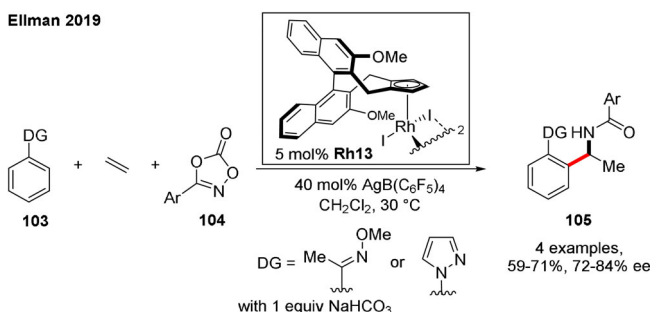


Scheme 22. Cp^xRh^{III}-catalyzed benzamide C–H bond addition to Michael acceptors.

catalyzed by the dimeric complex **Rh13**.^[61] In 2020, Wang and co-workers reported the synthesis of tricyclic hydrophenanthridinones **100** from *N*-methoxybenzamides **98** and quinones **99**.^[65a] Pre-catalyst S-Cp-**Rh14** allowed access to differently functionalized products **100** in good yields and moderate to high enantioselectivities. In this case, sacrificial amounts of the benzoquinone substrate (2 equiv used in the reaction) may oxidize the Cp^xRh^I pre-catalyst to the catalytically active Cp^xRh^{III} species. After the common C–H activation and migratory insertion steps, the authors propose the formation

of a 7-membered rhodacycle **101** which undergoes protonolysis delivering intermediate **102**. Then, an off-cycle intramolecular amide nucleophilic addition to the carbonyl affords the final product **100**. Related work involves the use of Cp^{*}Rh catalysts bearing chiral disulfonate ligands for enantioselective C–H functionalization. While interesting, this is beyond the topic of this Review.^[65b]

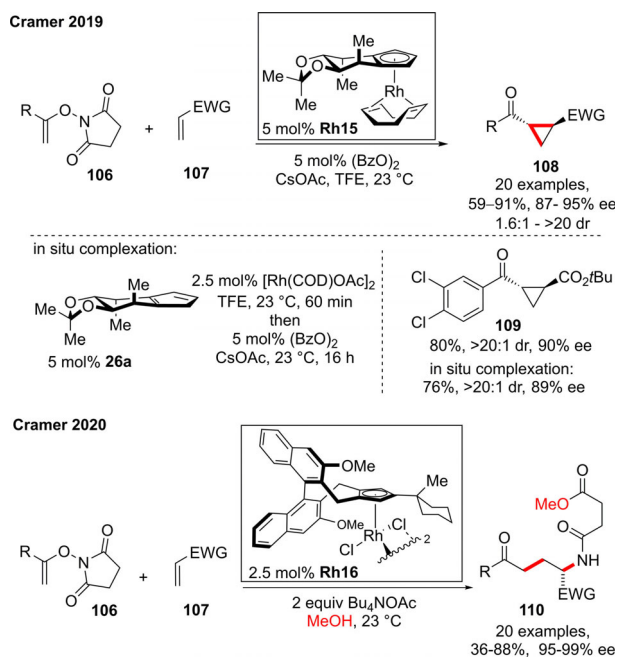
Ellman and co-workers demonstrated that, after C–H activation and olefin migratory insertion, cyclometalated rhodium species (as in **101**) can be trapped by a third component. They reported the enantioselective synthesis of a set of four α -methyl branched amides **105** from arenes **103** containing oxime or pyrazole directing groups, ethylene gas, and dioxazolones **104** as aminating reagents (Scheme 23).^[74] Using **Rh13** halide pre-catalyst activated with AgB(C₆F₅)₄ afforded products **105** in good yields and high enantioselectivity. We believe this first example of a Cp^xRh^{III}-catalyzed multicomponent reaction will serve as a source of inspiration for the future development of challenging transformations.



Scheme 23. Cp^xRh^{III}-catalyzed 1,1-addition of a C–H bond and aminating agent to ethylene.

Building upon racemic studies by Rovis,^[75] the Cramer group developed an asymmetric cyclopropanation reaction between *N*-enoxysuccinimides **106** and Michael acceptors **107** (Scheme 24).^[76] Pre-catalyst Mannitol-Cp**Rh15** was key to obtaining *trans*-cyclopropanes **108** in high yields, diastereo- and enantioselectivities. Noteworthy, complexes with other Cp^x ligand classes, such as BINOL-Cp or cPent-Cp, gave significantly lower reactivity and selectivities. The high synthetic utility of this transformation was demonstrated in the synthesis of monooxygenase inhibitor (UPF-648) precursor **109**, as well as cyclopropane building blocks of natural products. Remarkably, when the active catalyst was formed in situ from [Rh(COD)OAc]₂ and pre-ligand **26a**, comparable reactivity and selectivity to the standard protocol were obtained. Alternatively, the authors demonstrated later that by changing the catalyst from Mannitol-Cp**Rh15** to BINOL-Cp**Rh16**, and running the reaction in methanol instead of trifluoroethanol, carboamination acyclic products **110** were generated instead.^[77] A broad range of unnatural α -amino acids (EWG = CO₂R) were synthesized accordingly in moderate to high yields and with excellent enantioselectivity. Presumably, the MeOH solvent assists by nucleophilic ring-opening of the *N*-enoxysuccinimide substrate, being incorporated into the methyl ester products **110**.

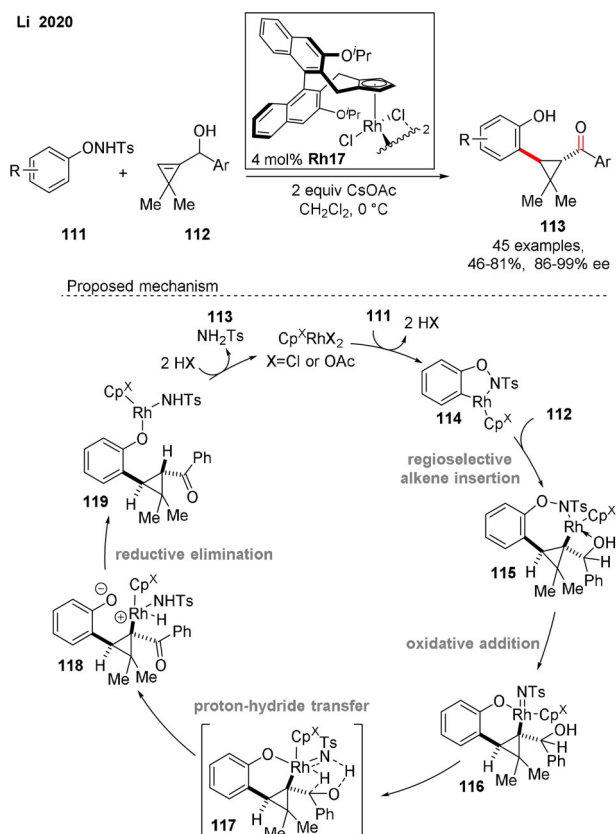




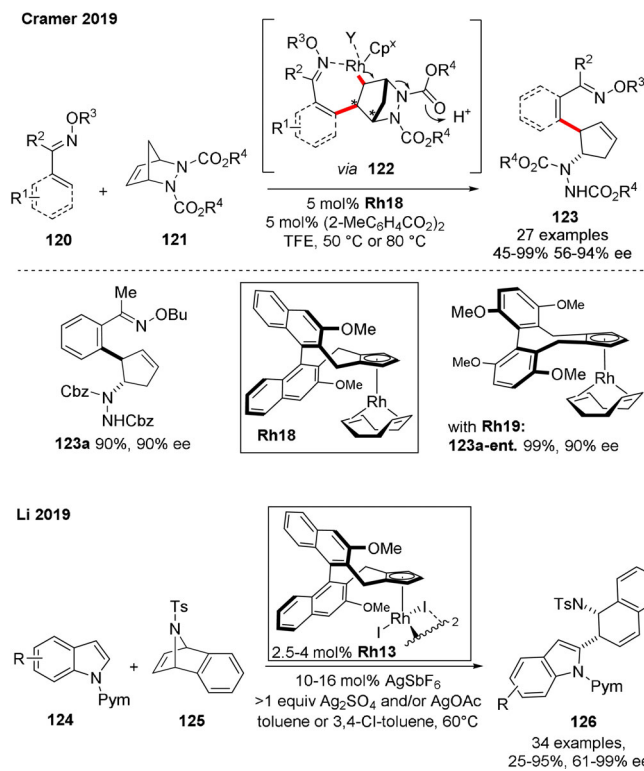
Scheme 24. Divergent Cp^XRh^{III}-catalyzed functionalization of *N*-enoxysuccinimides with Michael acceptors.

In 2020, Li and co-workers adopted a different strategy for the formation of chiral cyclopropanes, employing cyclopropenyl secondary alcohols **112** as ring-strained coupling partners (Scheme 25).^[78] They reported a redox-neutral diastereo- and enantioselective C–H cyclopropylation of *N*-phenoxy sulfonamides **111** using **Rh17** catalyst under mild reaction conditions. Based on experimental studies and DFT calculations, the authors suggested a reaction mechanism whereby C–H activation of **111** affords rhodacycle **114**. Subsequent regioselective and stereodetermining cyclopropane migratory insertion generates a 7-membered cyclic Rh^{III} species **115**. Oxidative addition into the N–O bond leads to a Rh^V nitrenoid species **116**, which undergoes proton-hydride transfer giving **118**. Finally, reductive elimination to **119** followed by protonolysis furnishes the *trans* cyclopropane product **113** and regenerates the catalyst.

Other Cp^XRh-catalyzed transformations to complex molecules having two consecutive stereogenic centers involve the fragmentation of strained bicyclic olefins. In 2019, Cramer et al. reported a C–H activation/ring-opening sequence of aryl and alkenyl oxime ethers **120** and diazabicycloalkenes **121** for the construction of cyclopentenyl amines **123** (Scheme 26).^[79] Differently substituted aryl oxime substrates were tolerated in high yields and enantioselectivities. Notably, the reaction scope could be extended to α,β -unsaturated oximes at higher temperatures, which constitutes one of the first examples of Rh^{III}-catalyzed functionalization of alkenyl C–H bonds. The proposed mechanism involves an enantio-determining *exo*-selective migratory insertion of the olefin leading to rhodacycle **122**. This undergoes anti- β -nitrogen elimination generating the desired product **123**. Remarkably, both the COD ligand of pre-catalyst **Rh18** and the aryl peroxide oxidant play a role in reactivity and enantioselectivity, but their exact contribution remains obscure. Later



Scheme 25. Cp^XRh^{III}-catalyzed C–H cyclopropylation of *N*-phenoxy sulfonamides.



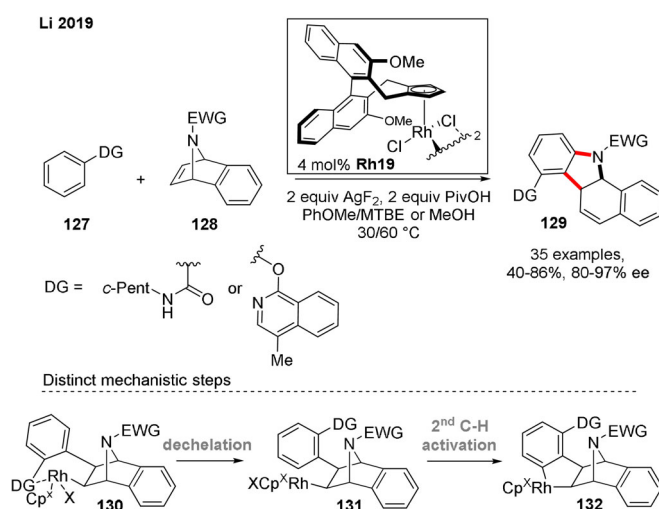
Scheme 26. Cp^XRh^{III}-catalyzed C–H functionalization with heterobicyclic olefins.

studies showed that pre-catalyst **Rh19**, bearing a bis-MeO-phenyl atropochiral Cp^X ligand, improved the reactivity while maintaining high stereocontrol in this transformation.^[44]

The same year, Li and co-workers developed a closely related C–H functionalization of *N*-pyrimidylindoles **124** with 7-azabenzonorbornadienes **125** using complex **Rh13** (Scheme 26).^[80] As in the previous example, the proposed mechanism involves a stereospecific β-nitrogen elimination. Depending on the substrate, a set of four different reaction conditions (toluene vs. 3,4-dichlorotoluene, Ag₂SO₄, and/or AgOAc) were used to access a variety of products **126** in high yields and enantioselectivities. Despite the redox-neutral character of the transformation, super-stoichiometric amounts of a silver oxidant were needed to ensure high reactivity. According to the authors, the silver additive may facilitate the C–H activation step and activate the olefin coupling partner.

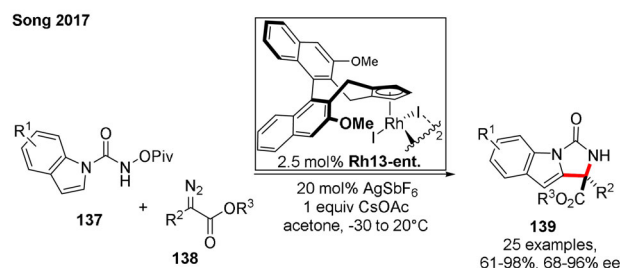
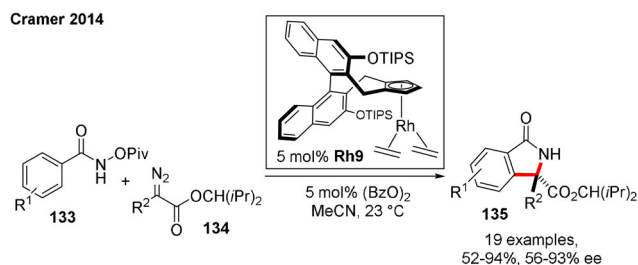
Later the Li group reported an enantioselective oxidative [3+2] annulation of arenes **127** with azabenzonorbornadienes **128** (Scheme 27).^[81] Two different directing groups (DG) were used on the arene coupling partner: *N*-cyclopentylamide and a designed (4-methyl)-1-isoquinolyl ether. The reaction was conducted using AgF₂ as stoichiometric oxidant, and different solvents and temperatures were chosen depending on the directing group. Based on KIE studies and stoichiometric experiments, the authors proposed a reaction mechanism involving two C–H activation events. A first *ortho* C–H activation of **127** followed by stereodetermining alkene *syn* migratory insertion (*cis* to the NTs group) generates rhodacycle **130**. After directing group dechelation (**131**), a second (*meta*) C–H activation gives rhodacycle **132**. This undergoes β-nitrogen elimination (as in intermediate **122**) and C–N bond forming reductive elimination to furnish a *cis*-fused dihydrocarbazole product **129**. According to the authors, a flexible DG was key to enabling the double C–H activation sequence via rhodium dechelation.

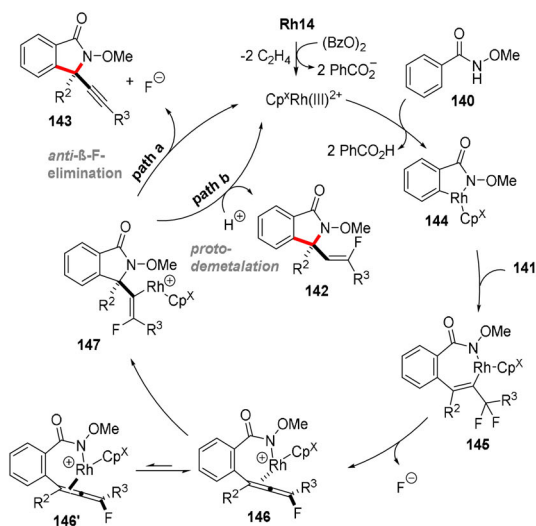
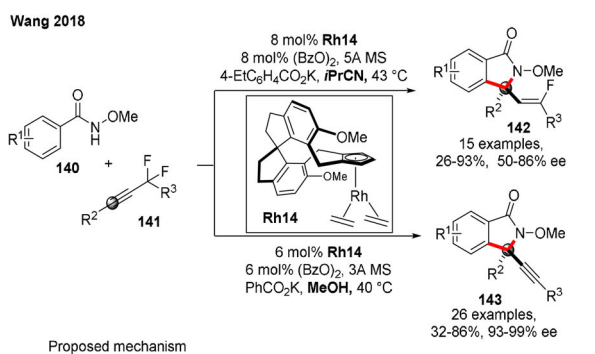
Cp^XRh^{III} catalysts have also been very efficient in the construction of tetrasubstituted carbon stereocenters by C–H



bond functionalization. A common approach involves the [4+1] annulation of arylhydroxamates with one-carbon electrophilic components, similar in mechanism to the previous [4+2] annulation reaction (Scheme 18). The first example was reported by the Cramer group, who employed pre-catalyst **Rh9** for the synthesis of chiral isoindolinones **135** from arylhydroxamates **133** and donor/acceptor diazo compounds **134** (Scheme 28).^[82] To ensure high enantioselectivity, the two substituents of **134** had to be different in size, with a bulky 3-(2,4-dimethyl-pentyl) ester group being optimal. The diazo insertion step was proposed as enantiodetermining, with the big ester substituent preferentially positioned away from the *O*-pivaloyl group of the hydroxamate (**136**). In 2017, Song and co-workers extended the [4+1] annulation scope to indolyl hydroxamates **137**.^[62] By employing the pre-catalyst **Rh13** (*S* enantiomer), activated with AgSbF₆ as halide abstractor, a range of differently decorated products **139** were prepared in high yields and enantioselectivities.

In 2018, Wang et al. disclosed the divergent synthesis of monofluoroalkenyl and alkynyl isoindolinones **142** and **143** by [4+1] annulation of *N*-methoxy benzamides **140** with propargyl difluorides **141** as atypical one-carbon component (Scheme 29).^[83] Catalyst optimization studies showed superior reactivity and enantioselectivity of the complex SCP-**Rh14** compared to analogs bearing BINOL-Cp^X ligands. Alkyne products **143** were synthesized in excellent enantioselectivities by using MeOH as solvent. Alternatively, *i*PrCN gave *Z*-monofluoroalkenyl isoindolinones **142** with moderate enantioselectivities. The authors propose the following reaction mechanism: Cyclometalation of **140** to **141** and regioselective alkyne migratory insertion result in rhodacycle **145**.

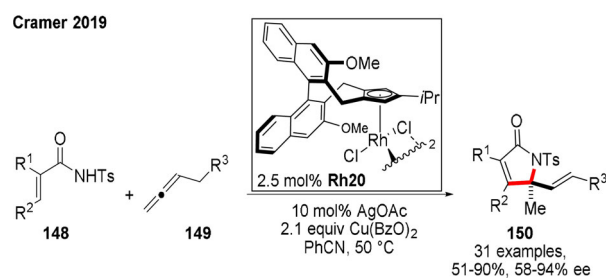




Scheme 29. Cp^XRh^{III}-catalyzed divergent synthesis of alkenyl and alkynyl isoindolones.

Then, a stereoselective fluorine elimination provides the chiral allene Rh complex **146**, which might be in equilibrium with the less favored facial isomer **146'**. Kinetic resolution by allene migratory insertion generates *E*-alkenyl Rh species **147**. From here, anti-β-F-elimination leads to alkyne product **143** (path a), whereas the *Z*-fluoroalkene product **142** is formed in the *i*PrCN system by protodemetalation (path b). In the MeOH system, rhodium intermediate **147** might be coordinated to benzoate anions, promoting an E1cB-like fluorine elimination. Hydrogen bonding between MeOH and F can also facilitate defluorination. Alternatively, the more strongly binding *i*PrCN might coordinate species **147** and thereby withdraw electron-density from the metal, thus favoring protodemetalation instead.

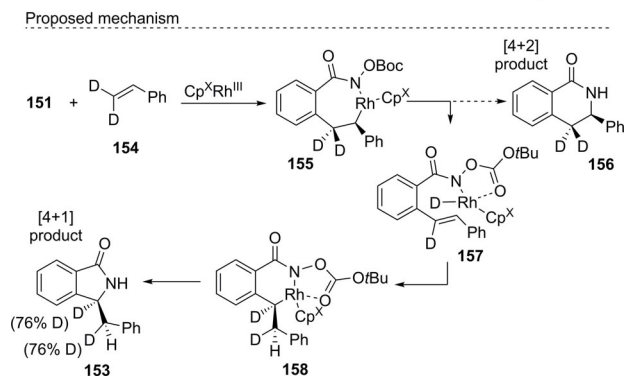
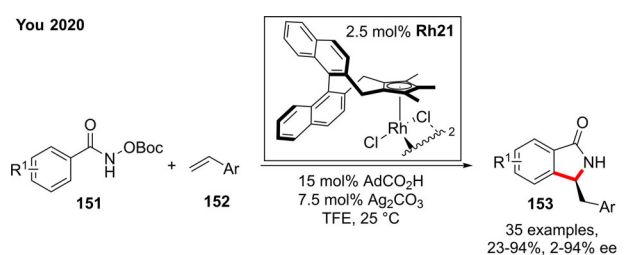
Unactivated alkenyl C–H bonds also engage in the [4+1] annulation reaction. In 2019, the Cramer group reported the enantioselective functionalization of acrylamides **148** with allenes **149** as one-carbon components for the generation of relevant α,β-unsaturated-γ-lactams **150** (Scheme 30).^[84a] In this case, **Rh20** pre-catalyst with a third substituent (*i*Pr) at the Cp ring was optimal to provide stereocontrol (up to 94% ee). Remarkably, the external stoichiometric oxidant had an influence in the reaction, with copper salts being superior to silver salts regarding their reactivity and selectivity. Among the first, Cu(OBz)₂ gave significantly higher enantioselectivities than Cu(OAc)₂. Later the methodology



Scheme 30. Cp^XRh^{III}-catalyzed [4+1] annulations of acrylamides and allenes.

was extended to acrylic acids leading to chiral γ-lactone products.^[84b]

The possibility of modulating reactivity and selectivity by altering the ligand's Cp ring substitution was further highlighted by You and collaborators, who recently applied Rh complexes of pentasubstituted Cp^X ligands to the synthesis of chiral isoindolinone products **153** via [4+1] annulation of benzamides **151** and styrenes **152** (Scheme 31).^[42] In comparison, analogous disubstituted Cp^XRh complexes were previously shown to yield exclusively [4+2] products (see Scheme 17). Based on isotopic labelling experiments, the authors proposed a reaction mechanism whereby the first steps leading to intermediate **155** are identical with the accepted ones in the [4+2] annulation. From here, while disubstituted Cp^X complexes favor reduction–elimination leading to **156**, pentasubstituted Cp^X**Rh21** favors β-syn migratory insertion to hydride species **157**. Subsequent alkene migratory insertion yields the stable 6-membered rhodacycle **158**, which was isolated and confirmed by x-ray analysis. Finally, stepwise C–N bond reductive elimination followed by N–O bond oxidative addition affords the desired isoindoli-



Scheme 31. Pentasubstituted BINOL-Cp^X ligands favor [4+1] isoindolinone annulation products by Rh^{III} catalysis.

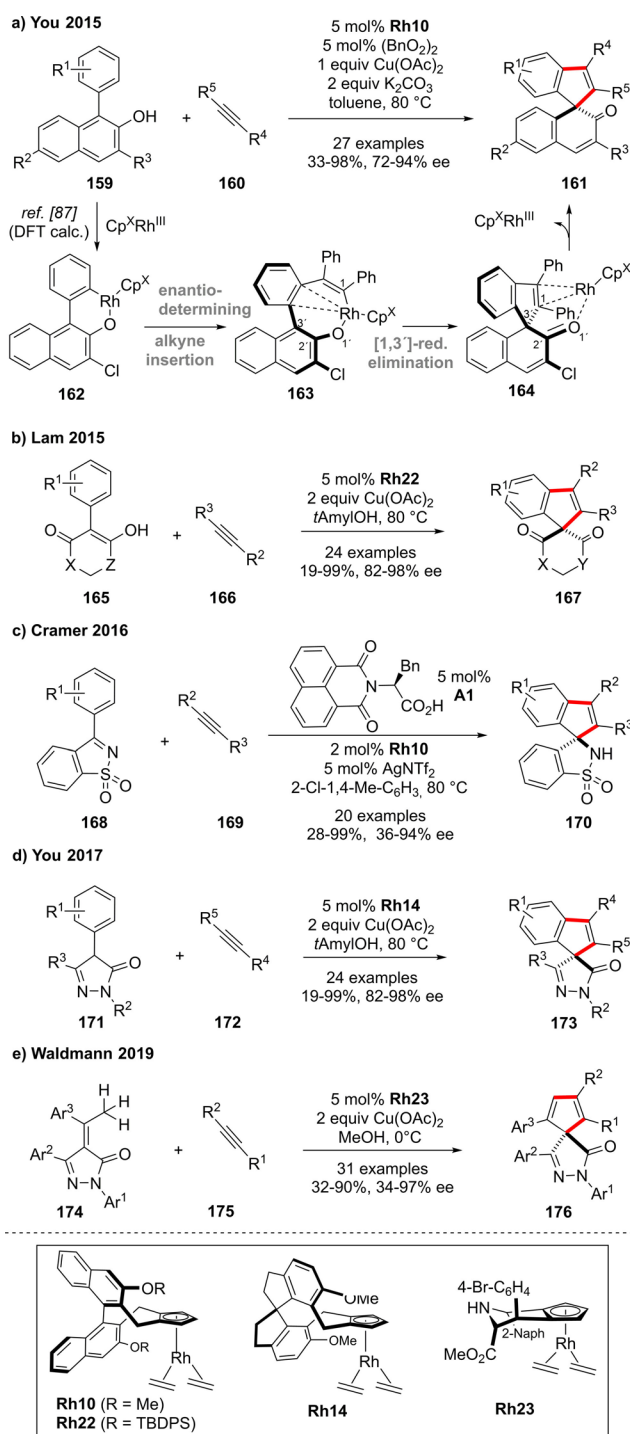
none product **153**. Overall, a broad range of benzamide and styrene coupling partners engaged in the reaction, providing **153** in generally high yields and enantioselectivities (up to 94% *ee*). Noteworthy, the presence of *ortho*-substituents (-OMe, -Ph) in the binaphthyl backbone of the pentasubstituted Cp^XRh catalyst was detrimental to reactivity.

Cp^XRh^{III} catalysts have also been applied to the challenging synthesis of chiral spiro compounds. Despite their unique 3D structural properties, this motif is underrepresented in pharmaceutical libraries.^[85] Four closely related [3+2] spiroannulations of alkynes with different C–H coupling partners have been disclosed (Scheme 32a). In 2015, the You group reported a phenol-directed dearomatization of β -naphthols **159** using BINOL-CpRh¹⁰ as pre-catalyst and Cu(OAc)₂ as stoichiometric oxidant.^[86] Spirocyclic enones **161** were synthesized in excellent levels of enantio- and regiocontrol from symmetrical and unsymmetrical alkynes **160**. Later mechanistic computational studies supported that, after the rate-limiting cyclometalation to **162**, an enantio- and regio-determining migratory alkyne insertion leads to an 8-membered axially chiral rhodacycle **163**.^[87] This species may be in equilibrium with a high-energy π -oxaallyl-Rh intermediate; however, only the η^1 -O-bound enolate undergoes reductive elimination generating the dearomatized intermediate **164**, from which the product is released.

In 2015, Lam and co-workers reported the annulation of enones **165** with BINOL-CpRh²² as pre-catalyst (Scheme 32b).^[43] The hydroxy-directed spiroannulation takes place in excellent regioselectivities when using unsymmetrical alkyl/(hetero)aryl-substituted alkynes **166**. Spiroindenes **167** containing ketoesters, ketolactams, or a barbiturate were generated in generally high enantioselectivities. In 2016, the Cramer group extended the repertoire of nucleophilic partners to *N*-sulfonyl ketimines **168**, leading to spirocyclic sultams **170** (Scheme 32c).^[88] Catalyzed by BINOL-CpRh¹⁰, the reaction was most efficient in the presence of *L*-phenylalanine-derived acid **A1** and AgNTf₂ as oxidant in a peculiar chlorinated solvent at 80 °C. Noteworthy, the chirality of the carboxylic acid has no influence on enantioselectivity, and the same results were obtained using the *D* enantiomer. In contrast to the previous reports, unsymmetrical alkyl/aryl alkynes reacted in low regioselectivities.

In 2017, You et al. employed S-CpRh¹⁴ for the synthesis of spiropyrazolones **173** in the presence of Cu(OAc)₂ as stoichiometric oxidant (Scheme 32d).^[89] Noteworthy, catalyst BINOL-CpRh¹⁰ provided the same levels of reactivity and enantioselectivity. A series of 4-aryl-5-pyrazolones **171** were tolerated, producing **173** in high to excellent yields and enantioselectivities. According to the authors, the transformation proceeds via pyrazolone-enolate-directed C–H activation. This methodology was later extended by the Waldmann group to the annulation of α -arylidene pyrazolones **174** through formal C(sp³)-H activation (Scheme 32e).^[90] A new JasCpRh²³ complex bearing a naphthyl substituent provided spirocycles **176** in moderate to excellent enantioselectivities at low temperature.

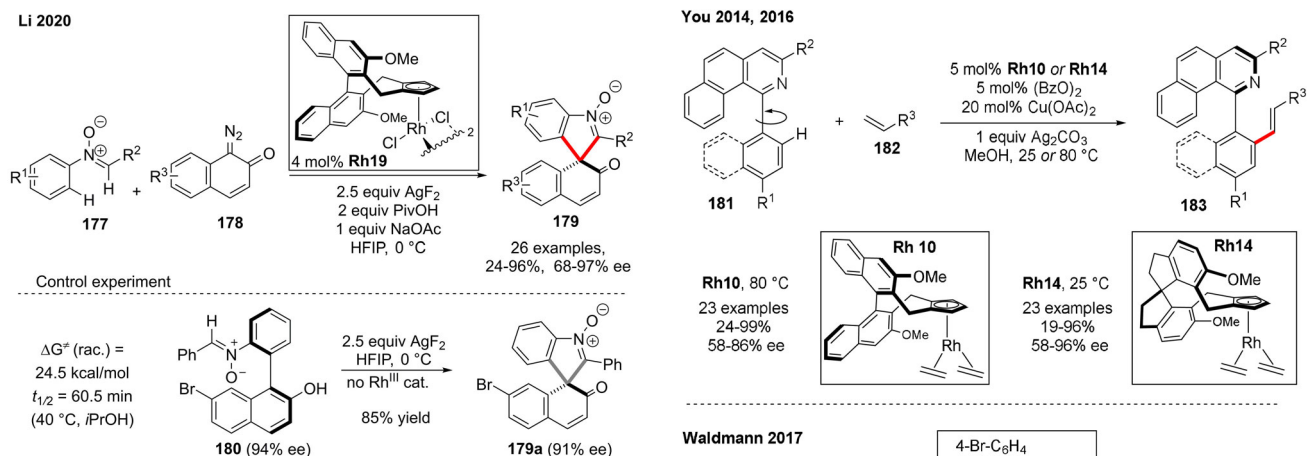
The most recent enantioselective synthesis of spirocycles came from the Li group, who envisioned an asymmetric [4+1] annulation between *N*-aryl nitrones **177** and quinone diazides



Scheme 32. Cp^XRh^{III}-catalyzed [3+2] spiroannulation with alkynes as coupling partner.

178 via axial-to-central chirality transfer (Scheme 33).^[91] Using **Rh19** as pre-catalyst and AgF₂ as stoichiometric oxidant afforded spironitrones **179** in excellent yields and enantioselectivities at 0 °C. The rotational barrier of bis-arene reaction intermediate **180** was calculated to be 24.5 kcal mol⁻¹ at 40 °C, indicating an atropomeric metastability. From **180**, the corresponding spironitronone product **179a** could be obtained with a high level of chirality transfer in the absence





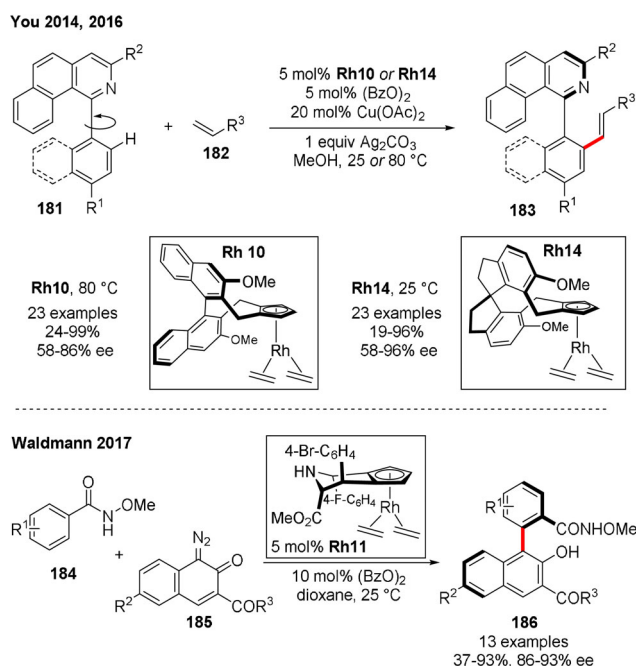
Scheme 33. Cp^XRh^{III}-catalyzed [4+1] spiroannulation of nitrones with diazo acceptors.

of the rhodium catalyst, presumably via an oxidative radical cyclization mechanism.

The metal-catalyzed asymmetric C–H functionalization of arenes constitutes one of the most efficient strategies towards the synthesis of axially chiral biaryls.^[92] The direct forging of a chiral biaryl axis is a challenging task. In order to maintain high enantiopurity, a high rotational stability is mandatory. For that, a total minimum of three *ortho*-substituents is typically required on the two aromatic coupling partners, generating a hindered environment around the metal center, which potentially hampers reactivity. The usually required elevated temperatures complicate achieving high enantiocontrol. An alternative strategy relies on the insertion of a substituent onto a preexisting freely rotating biaryl axis, with the rotational barrier energy increasing upon addition of the extra substituent. Notably, Cp^XRh^{III} complexes (and Cp^XIr^{III}; Scheme 39) have proven to be efficient catalysts in the synthesis of axial-chiral biaryl scaffolds by these two conceptually different strategies.

In 2014, the You group reported the first example via dehydrogenative coupling between pre-formed biaryl derivatives **181** and alkenes **182** (Scheme 34).^[93] Using a BINOL-CpRh^{III} complex, a library of 23 alkenylated heterobiaryls **183** was produced in high yields and enantioselectivities. The reaction follows a traditional Heck mechanism. Noteworthy, the arene C–H activation step, forming a 5-membered cyclometalated species, requires the coplanarity of two sterically hindered arenes, which raises the reaction energy barrier. The reaction scope was later extended to polyaromatic styrenes as well as differently substituted heterobiaryls by using SCpRh^{III} as catalyst,^[45] which, remarkably, allowed lower reaction temperatures.

In 2017, Waldmann et al. reported the construction of atropochiral biaryl compounds by C–H functionalization of hydroxamide-derived arenes **184** with diazonaphthoquinones **185** as carbene precursors (Scheme 34).^[46] With the aid of the JasCpRh^{III} complex, a set of 13 densely functionalized biaryls **186** were obtained in high yields and excellent enantioselectivities. The same group later published a JasCp-Rh^{III}-catalyzed intramolecular atroposelective [4+2] annulation

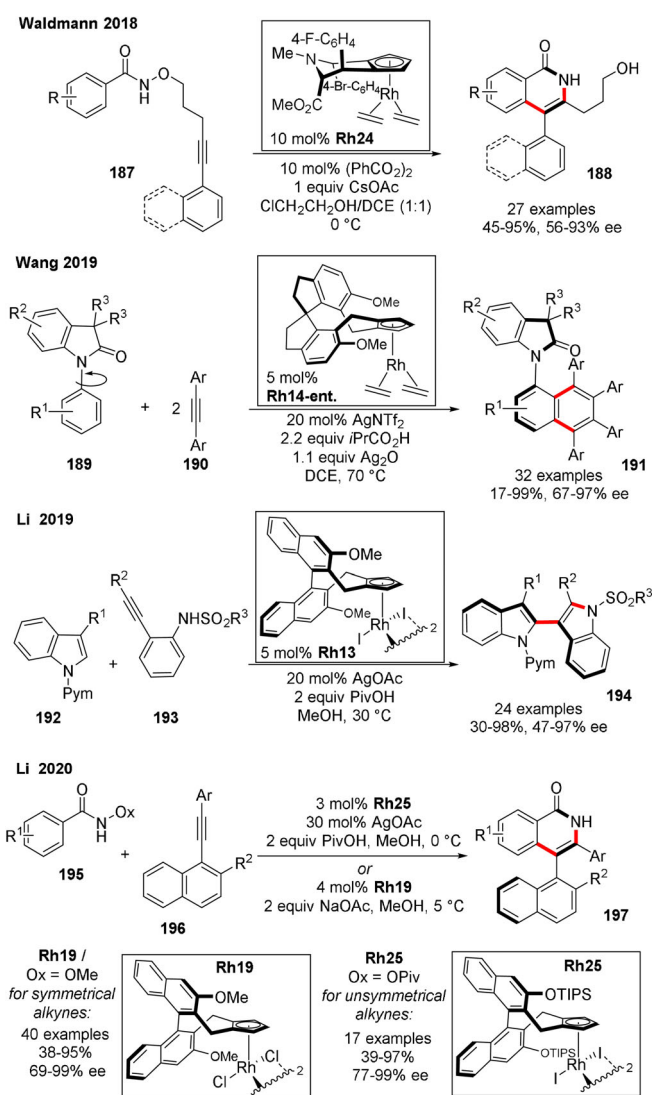


Scheme 34. Cp^XRh^{III}-catalyzed atroposelective C–H functionalization with alkene and diazo acceptors.

of hydroxybenzamide derivatives tethered to naphthyl-substituted alkynes **187**, forming axially chiral 4-aryloxyquinolones **188** in high yields and enantioselectivities (Scheme 35).^[94a]

In 2019, Wang and co-workers published the enantioselective synthesis of C–N axially chiral *N*-aryloxindoles **191** by a Satoh-Miura-type 2-fold C–H activation of *N*-aryloxindoles **189** and coupling with two units of diaryl alkynes **190**.^[94b] The combination of the pre-catalyst SCpRh^{III}-ent. and stoichiometric amounts of silver isobutyrate (*i*PrCO₂Ag), generated in situ from *i*PrCO₂H and Ag₂O, was optimal for high enantioselectivity and reactivity in the process. Presumably, a bulky acid provides better stereocontrol in the initial carboxylate-assisted C–H activation event. Whereas high enantioselectivity was maintained with asymmetric diaryl alkyne partners, practically no regioselectivity was observed.

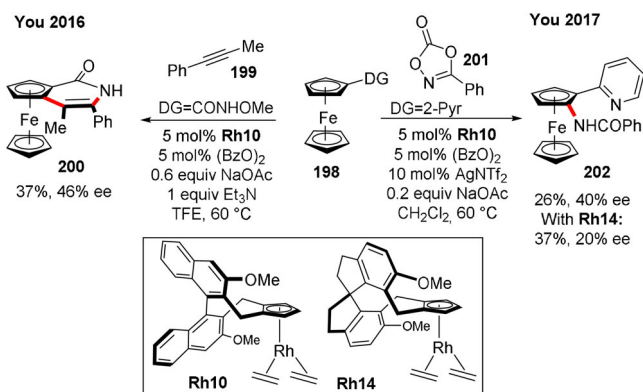
The same year, the Li group tackled the challenging atroposelective synthesis of biindoyls (Scheme 35).^[95] With the highly active catalyst Rh^{III}, a broad range of 2,3'-disubstituted biindoyl products **194** were accessed in modest to excellent yields and high enantioselectivities from substrates **192** and **193** via C–H activation/indole nucleophilic cyclization. Control experiments showed no reaction between a pre-formed indole and different pyrimidyl-indoles **192**, which indicated that a Rh^{III} indoyl intermediate was the active species instead of a protonolyzed indole. Remarkably, the rhodacycle formed after C–H activation could be isolated and characterized by x-ray analysis, corroborating the stereochemical model originally proposed by Cramer (Scheme 18b). More recently, Li and co-workers reported the use of BINOL-Cp complexes Rh^{III} and Rh^{III} to form atropochiral isoquinolinones **197** by C–H activation of aryl hydroxamates **195** followed by [4+2] annulation with alkynes **196**



Scheme 35. $\text{Cp}^*\text{Rh}^{\text{III}}$ -catalyzed atroposelective C–H functionalization with alkyne acceptors.

(Scheme 35).^[96] Mechanistically, the hydroxamate cyclometalation is followed by an enantiodetermining alkyne migratory insertion. Then, an axial-to-axial chirality transfer process leads to the products **197**. Both symmetric and non-symmetric bulky alkyne partners were successful, depending on the choice of catalyst, which gave access to a broad library of products **197** in excellent yields, regio- and enantioselectivities.

Like chirality, planar chirality has also been controlled by Cp^*Rh complexes. In 2016, the You group extended the [4+2] annulation with alkynes to ferrocenes bearing a carboxamide as directing group **198** (DG = CONHOMe) (Scheme 36, left).^[97] Building upon racemic studies, the feasibility for an asymmetric reaction was demonstrated with one example using BINOL-CpRh**10** as pre-catalyst. Under unoptimized conditions, ferrocene-based pyridinone **200** was obtained as a single regioisomer in moderate yield and enantioselectivity. Later the same group showed one other example of enantioselective C–H amidation of ferrocenylpyridines **198** (DG = 2-



Scheme 36. $\text{Cp}^*\text{Rh}^{\text{III}}$ -catalyzed ferrocenyl C–H functionalization; generation of planar chirality.

Pyr) with dioxazolones **201** as masked *N*-acyl nitrenes transfer reagents (Scheme 36, right).^[98] Both $\text{ScP}^*\text{Rh14}$ and BINOL-CpRh**10** provided planar chiral ferrocene in moderate yields and enantioselectivities, with the latter providing a slightly higher enantiocontrol. These two preliminary investigations constitute a proof of concept for the generation of planar chirality under Cp^*Rh catalysis.

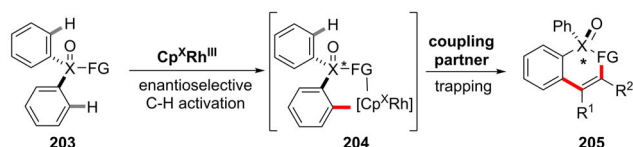
Compared to the enantioselective creation of carbon stereogenic centers, the synthesis of chiral-at-heteroatom molecules through asymmetric C–H functionalization remains underdeveloped.^[99] Chiral phosphorous(V) compounds play a key role as ligands in asymmetric catalysis.^[100] Chiral sulfur(VI) compounds are ubiquitous in nature and of high interest in the pharmaceutical and agrochemical industries.^[101] In this regard, different Cp^*Rh complexes have been successfully applied in the enantioselective synthesis of these scaffolds making use of the functionality attached to the heteroatom as a directing group. A common synthetic approach involves the desymmetrization of prochiral substrates **203** by enantiodetermining C–H activation (Scheme 37a). The resulting rhodacycle **204** is intercepted by a coupling partner leading to cyclic chiral products **205**.

In 2017, Cramer and co-workers presented an asymmetric synthesis of *P*-chiral cyclic products **208** by desymmetrization of phosphinamides **206** with internal alkynes **207** using the pre-catalyst **Rh10** (Scheme 37b).^[102] This is the first example of a Rh^{III} -catalyzed enantiotopic C–H activation. The use of one equivalent of K_2CO_3 in combination with Ag_2CO_3 as stoichiometric oxidant was key to obtaining high enantioselectivities towards products **208**. Other bases such as KH_2PO_4 were inferior. Notably, the transformation was applicable to differently functionalized symmetrical and unsymmetrical alkynes, and a superior regioselectivity was obtained with $\text{Cp}^*\text{Rh10}$ compared to the analogous achiral Cp^* complex. Mechanistic deuterium exchange experiments performed by the authors revealed higher deuteration of **206** in the absence of K_2CO_3 , suggesting that the base is key to reducing the reversibility of the enantiodetermining C–H activation step.

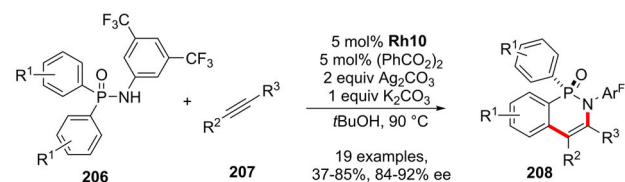
In 2018, the Cramer group and the Li group independently reported a desymmetrizing [4+2] annulation of diaryl sulfoximines **209** with α -ketodiazoo compounds **210**, affording chiral-at-sulfur 1,2-benzothiazines **211** (Scheme 37c). Exten-



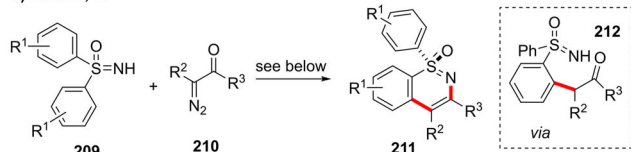
a) Creation of heteroatom (X) stereocenters by desymmetrization



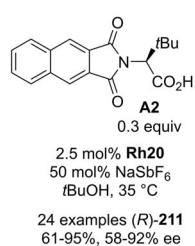
b) Cramer 2017



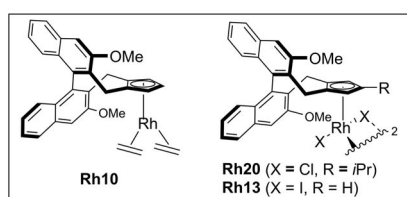
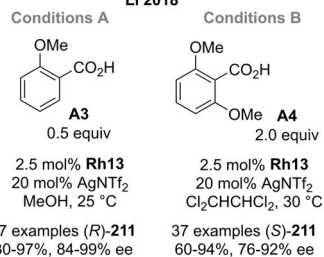
c) Cramer, Li



Cramer 2018



Li 2018



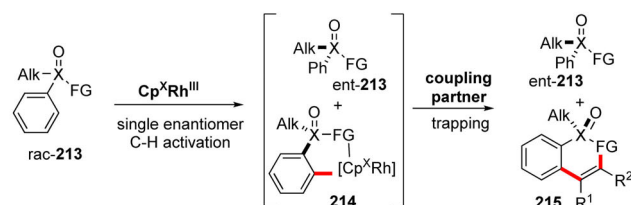
Scheme 37. Cp^xRh^{III}-catalyzed generation of *P*- and *S*-chiral stereocenters by desymmetrization.

sive optimization studies by the Cramer group^[103] showed that the stereoselectivity of the transformation was sensitive to the carboxylic acid, the Rh-complex, and the solvent. In one example, when hexafluoro-2-propanol (HFIP) was used instead of *t*BuOH, the opposite enantiomer of the product was obtained. Cp-trisubstituted **Rh20** catalyst in combination with *tert*-leucine-derived chiral acid **A2** in *t*BuOH gave products **211** in high yields and enantioselectivities. A variety of diazo coupling partners **210** were successful, including acceptor/acceptor substituents and α -ketone solely. Less reactive diazo compounds led to decreased enantioselectivity, possibly by increasing the reversibility of the enantiodetermining C–H activation step. After cyclometalation, the authors proposed a carbenoid insertion and protonation to produce ketone intermediate **212**. An off-cycle condensation delivers the desired product. Complementarily, Li and co-workers employed **Rh13** as catalyst combined with achiral

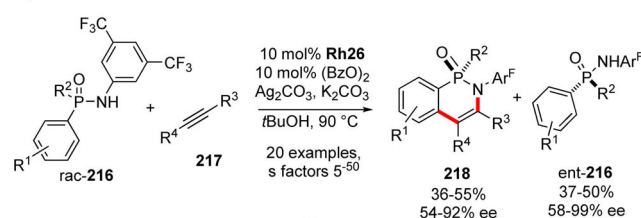
carboxylic acids.^[104] Whereas 2-methoxybenzoic acid **A3** in MeOH solvent (Conditions A) resulted in the *R* enantiomer of the products, 2,6-dimethoxybenzoic acid **A4** in tetrachloroethane afforded the *S* enantiomer. A broad scope of benzothiazines **211** were accessed in high yields and enantioselectivities.

An intrinsic feature of the desymmetrization strategy is the limited applicability to substrates bearing identical substituents. However, this can be overcome by the kinetic resolution of racemic substrates (Scheme 38a). In that case, the Rh^{III} catalyst reacts at different rates with each enantiomer of the substrate *rac*-**213**. Ideally, only one reacts (**214**), generating the desired product **215** in up to 50% yield. The remaining starting material *ent*-**213** is enantioenriched. In 2018, the Cramer group applied this strategy to phosphinic amides **216** (Scheme 38b).^[41] The design of a new trisubstituted Cp^x ligand class led to higher starting material enantio-discrimination. Whereas standard **Rh10** gave moderate *s* factors and enantioselectivities (*s* 14, 82% *ee* *ent*-**216**, 70% *ee* **218**), **Rh26**, featuring a large *tert*-butyl group on the Cp ring, afforded *s* values of up to 50 (99% *ee* *ent*-**216**, 92% *ee* **218**). Different aryl or alkyl substituents on the phosphinic amides **216** were successful. Unsymmetrical internal alkynes **217** were also incorporated in a highly regioselective manner.

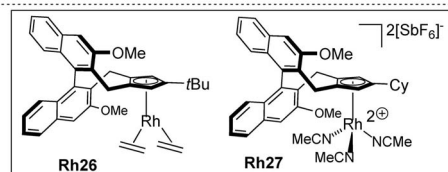
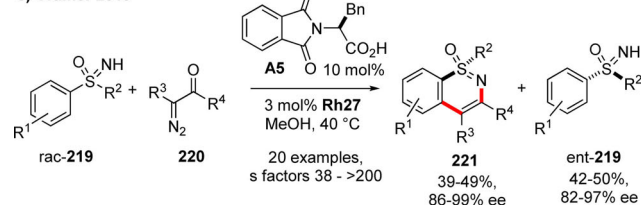
a) Kinetic resolution of heteroatom (X) stereocenters



b) Cramer 2018



c) Cramer 2019



Scheme 38. Cp^xRh^{III}-catalyzed kinetic resolution of *P* and *S* stereocenters.

Further, Cramer and collaborators extended the kinetic resolution methodology to aryl alkyl sulfoximines **219**, obtaining cyclic benzothiazine products **221** and enantio-enriched **219** by coupling with different diazo interceptors **220** (Scheme 38c).^[60] The symbiosis between the phenylalanine-derived acid **A5** and the trisubstituted-at-Cp catalyst **Rh27** enabled a strong kinetic enantiomeric differentiation of *rac*-**219**, providing *s* values greater than 200. The formal synthesis of two kinase inhibitors could be also accomplished.

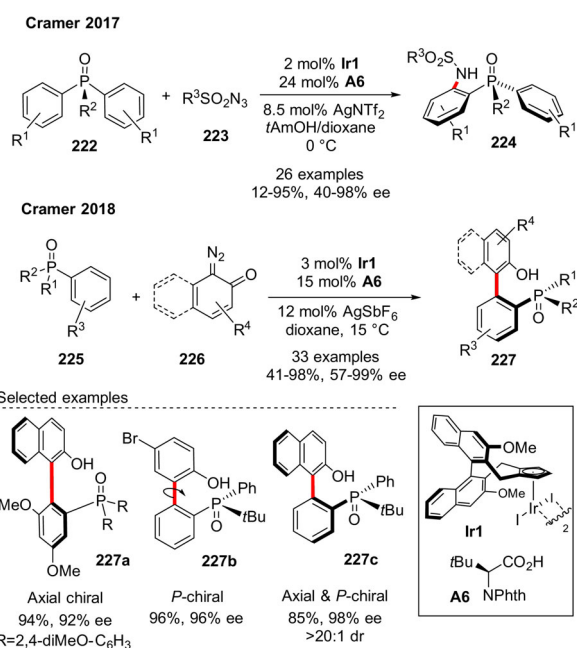
In this context, it should be mentioned that enantioselective C–H functionalizations have been also achieved with the aid of achiral Cp^{*}Rh catalysts in combination with chiral carboxylic acids. The interested reader can find examples elsewhere.^[9a,105,106]

4.3. Ir^{III} Catalysis

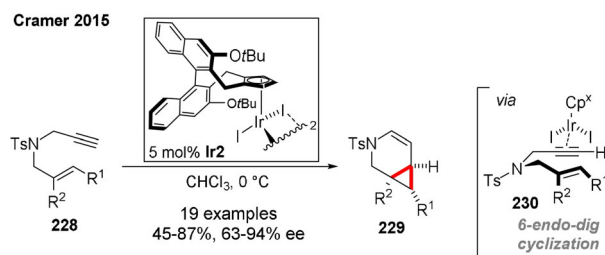
Iridium catalysis with chiral Cp^x ligands has been recently proven to be a powerful tool that enables challenging enantioselective transformations. This art remains in its infancy compared to more numerous related Rh-catalyzed transformations. Often both group-9 transition metals display unique reactivity. Nevertheless, Cp^xIr complexes may constitute an effective alternative to the more expensive rhodium analogs. For example, in the context of enantioselective C–H activation via a CMD mechanism, the combination of achiral Cp^{*}Ir catalysts with chiral acids has led to limited levels of enantioinduction.^[107] Here, the combination of chiral Cp^xIr complexes and chiral carboxylic acids offers an effective solution.

In 2017, the Cramer group developed an enantioselective desymmetrization of aryl phosphine oxides **222** through C–H amidation with sulfonfyl azides **223** (Scheme 39).^[108] The cooperation between complex BINOL-CpIr**1** and phthaloyl *tert*-leucine chiral carboxylic acid **A6** was key to achieving high reactivity and enantioselectivity towards valuable chiral-at-phosphorus products **224**. In comparison, low enantioselectivity (30% *ee*) was obtained when pairing **Ir1** with pivalic acid. Poor reactivity and enantioinduction (<5% yield, 4% *ee*) were likewise observed with chiral acid **A6** + achiral Cp^{*}Ir. A match/mismatch effect was observed between the enantiomers of **Ir1** and **A6**. The reaction scope was later enlarged to quinone diazide acceptors **226**.^[109] Using the same catalytic system, a diverse library of chiral phosphine oxides **227** was readily accessed in high yields and enantioselectivities featuring axial chirality (**227a**), *P* chirality (**227b**), or both (**227c**).

Beyond C–H functionalization chemistry, Cp^xIr complexes have shown a tremendous versatility and power, providing high stereocontrol by themselves. In 2015, the Cramer group developed BINOL-CpIr**2** and demonstrated its utility in the asymmetric intramolecular cycloisomerization of enynes **228**; for example, they were able to access challenging dehydropiperidine-fused cyclopropanes **229** (Scheme 40).^[56] The presence of bulky *tert*-butoxy *ortho* substituents on the Cp^x ligand was critical for high enantioselectivities, with the standard bis-MeO analog **Ir1** providing significantly lower stereoinduction (92 vs. 70% *ee*). Concep-



Scheme 39. Cp^xIr^{III}-catalyzed synthesis of axial and/or *P*-chiral phosphine oxides via C–H functionalization.



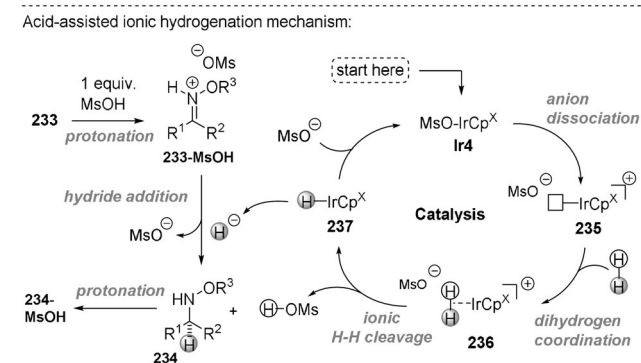
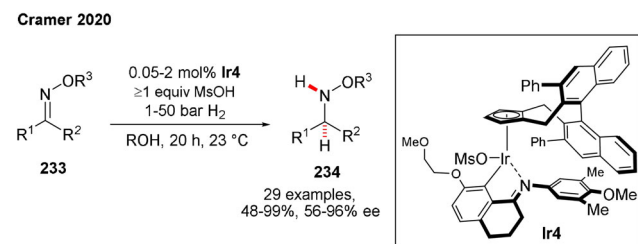
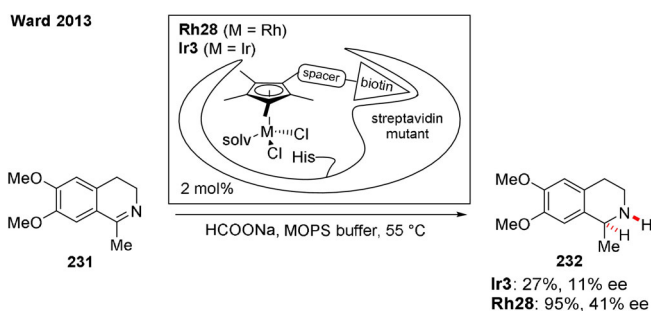
Scheme 40. Cp^xIr^{III}-catalyzed synthesis of fused cyclopropanes via enyne cyclization.

tually, the Cp^xIr^{III} catalyst shows Lewis acid reactivity more common to other noble metals (Au, Pt),^[110] activating the alkyne moiety towards internal alkene nucleophilic attack (intermediate **230**). The authors proposed that the orientation between the terminal alkyne and the Cp^x ligand determines the selectivity.

The reactivity of Cp^xIr complexes has been extended to important asymmetric hydrogenations.^[111] The Ward group explored the use of streptavidin-enzyme-linked Cp^x metal complexes for the enantioselective reduction of imine **231** by transfer hydrogenation (Scheme 41).^[112] Whereas iridium metalloenzyme **Ir3** achieved only low levels of conversion (27%) and enantioselectivity (11% *ee*) toward the tetrahydroisoquinoline product **232**, the rhodium analog **Rh28** showed improved catalytic performance (95% conv., 41% *ee*) under identical reaction conditions.

Recently, Cramer and collaborators developed a bench-stable cyclometalated Cp^xIr^{III} complex **Ir4**, which enabled the hydrogenation of challenging oximes **233** to valuable *N*-alkoxy amines **234** in high yields and enantioselectivities (Scheme 42).^[113] Notably, the reaction is fully chemoselective towards reduction of the oxime C=N bond and shows no





Scheme 42. Cyclometalated-Cp^XIr^{III}-catalyzed enantioselective hydroxylamine synthesis via oxime hydrogenation.

reductive cleavage of the weak N–O bond. The addition of stoichiometric amounts of a strong Brønsted acid (methanesulfonic acid = MsOH), was key to achieving high catalytic efficiencies (up to 4000 TON at room temperature). Based on this observation, the authors proposed an acid-assisted ionic hydrogenation mechanism,^[114] whereby the enantiodetermining facial-selective hydride transfer occurs from Cp^XIr hydride species **237** to the unbound protonated oxime substrate **233-MsOH**. The iridium hydride is formed from the pre-catalyst **Ir4** by dissociation of the methanesulfonate anion, facilitating dihydrogen coordination (**236**), and its subsequent ionic cleavage into a proton and a hydride source (MsOH and **237**, respectively). The generated MsOH protonates the basic hydroxylamine product **234** preventing catalyst poisoning. Noteworthy, the catalyst's supporting achiral C,N-chelate is key for reactivity and selectivity.

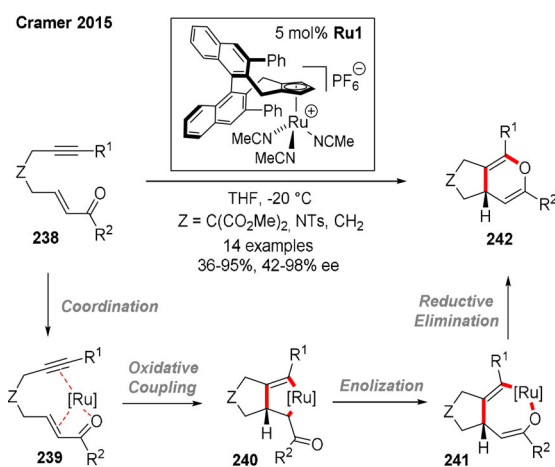
4.4. Ru^{II} Catalysis

Cyclopentadienyl Ru^{II} complexes have effectively catalyzed numerous diverse synthetic transformations.^[115,116]

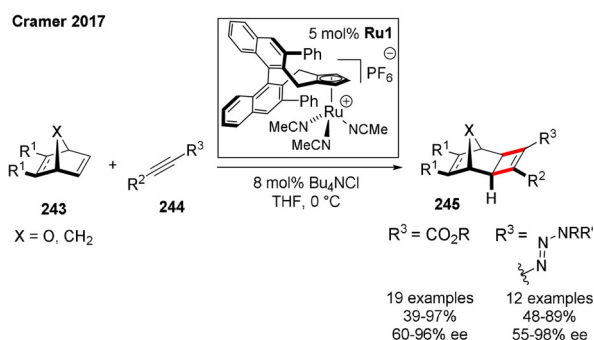
When the reactions require less than three available coordination sites at the metal center, strategies to achieve catalyst enantiocontrol include: i) tethering the Cp ring with another ligand, generating point or planar chirality,^[31,32] ii) the use of an exogenous source of chirality (e.g. chiral diphosphine).^[28] Complementarily, cationic Cp^XRu^{II} complexes, which present three available binding sites, offer an elegant solution for transformations demanding greater than two coordination sites.^[117]

In 2015, the Cramer group published a formal hetero Diels–Alder cyclization of yne-enones **238** to produce valuable chiral pyrans **242** (Scheme 43).^[51] The use of cationic BINOL-Cp^XRu^{II} catalyst **Ru1**, bearing phenyl *ortho* substituents as the Cp ligand sidewall, resulted in high reactivity and enantioselectivity at low reaction temperature. According to the proposed mechanism, three coordination sites of **Ru1** are required in the isomerization of a C-bound to an O-bound ruthenium enolate (**240** to **241**). Moreover, the difference in selectivity and reactivity observed when replacing the non-coordinating hexafluoroantimonate counterion of the complex (98% yield, 73% ee (*S*)) by a binding chloride (13% yield, 44% ee (*R*)) supports this hypothesis.

The versatility of catalyst **Ru1** was later demonstrated by the same group in related intermolecular [2+2] cycloadditions between strained norbornene derivatives **243** and internal alkynes **244** (Scheme 44).^[118] In contrast to the previous example, here the in situ occupation of one catalyst coordination site was key for high enantioselectivity towards *exo*-cyclic cyclobutenes **245**. The cationic catalyst **Ru1** itself showed excellent reactivity (98% yield in 1 h at 0 °C), but no stereoinduction. However, adding equimolar amounts of tetrabutylammonium chloride (Bu₄NCl) as a chloride source boosted the enantioselectivity (up to 98% ee). Other anions or neutral phosphine ligands were detrimental to reactivity and/or selectivity. The authors postulated that rapid binding of Cl[−] to **Ru1** generates a neutral [Cp^XRuCl] species, a chiral analog of the active Cp^{*}Ru(COD)Cl catalyst,^[119] which allows only one alkene and alkyne substrate to approach the metal center. The chiral environment provided by the BINOL-Cp^X ligand ensures a highly ordered transition state.



Scheme 43. Cp^XRu^{II}-catalyzed pyrane synthesis via [4+2] yne-enone cyclization.



Scheme 44. $\text{Cp}^*\text{Ru}^{\text{II}}$ -catalyzed synthesis of cyclobutenes via [2+2] cycloaddition.

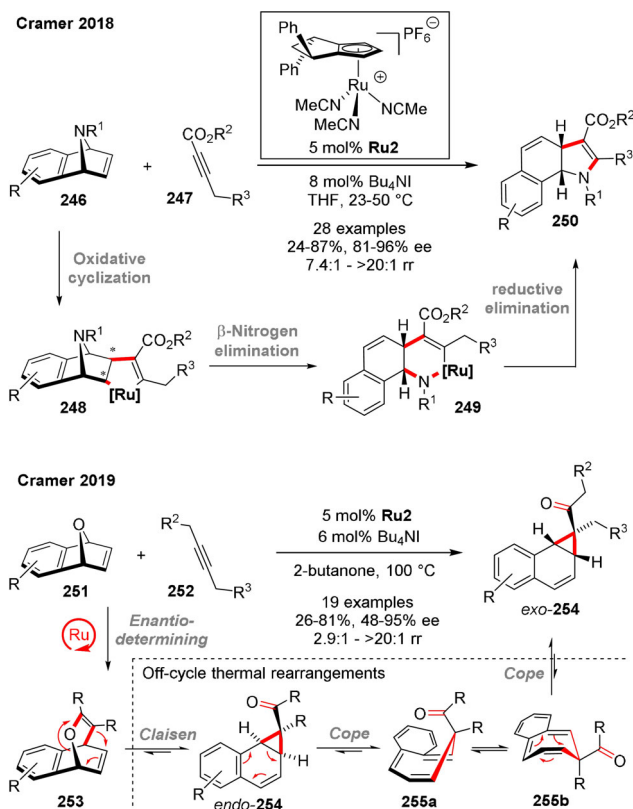
Importantly, the neutral catalyst could be recovered upon addition of norbornadiene at the end of the reaction, and re-engaged in catalysis.

Regarding the reaction scope, free acid or ester substituents on the alkyne **244** ($\text{R}^3 = -\text{CO}_2\text{R}$) were tolerated, the second providing better enantioselectivity. An oxygen bridge ($\text{X} = \text{O}$) was accepted albeit in lower enantioselectivity. Later the alkyne substrate scope was expanded to 1-alkynyl triazenes ($\text{R}^3 = -\text{N}_3\text{RR}'$), bearing alkyl substituents at the nitrogen atom.^[120] The corresponding alkenyltriazene products **245** were then used as vinyl cation surrogates. Under acidic conditions, a broad range of nucleophiles were inserted, giving access to different useful functionalities.

In 2018, the Cramer group extended the scope of the strained alkene from oxabicycles **243** to azabenzonorbornadienes **246** (Scheme 45). The latter reacted with alkynes **247** to give chiral dihydrobenzoindoles **250** upon in situ generation of a neutral $\text{Cp}^*\text{Ru}^{\text{I}}$ catalyst from cationic **Ru2** and tetrabutylammonium iodide.^[47a] In contrast to the previous example, [2+2] cyclization products (e.g. **245**) were not obtained. Instead, after the initial enantiodetermining oxidative cyclization step, the generated ruthenacycle **248** may undergo a sequence of stereospecific β -nitrogen elimination (**249**)/reductive elimination to **250**. Remarkably, chiral cPent-Cp ligands outperformed BINOL-Cp ligands in both reactivity and enantiocontrol. An identical trend was later observed in the development of an asymmetric synthesis of relevant benzonorcaradienes *exo*-**254** from oxabenzonorbornadienes **251** and alkynes **252**.^[121] Based on experimental and computational studies, the authors propose a mechanism whereby first a $\text{Cp}^*\text{Ru}^{\text{II}}$ -catalyzed enantioselective alkyne insertion affords high-energy allyl vinyl ether intermediate **253**. Subsequently, Claisen rearrangement affords an isolable *endo*-isomer **254**, which upon thermal isomerization by 6π -electrocyclic ring-opening/closure sequence leads to the thermodynamically more stable *exo*-**254**.

4.5. Co^{III} Catalysis

In recent years, catalysts based on abundant 3d-metals (Fe, Co, Ni, Cu, ...) have drawn significant interest driven by their lower price and toxicity compared to precious metals.^[122] While sometimes competing in efficiency, 3d-metal com-

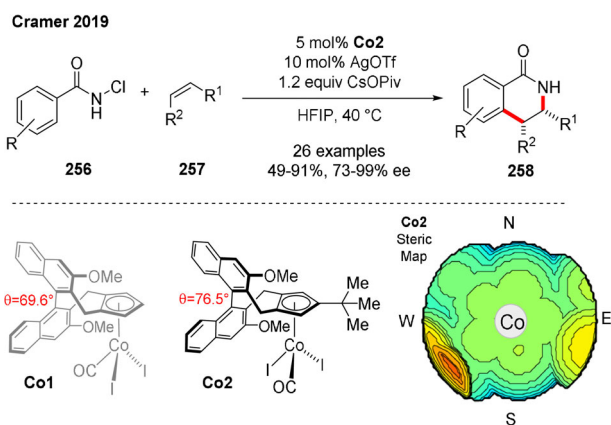


Scheme 45. $\text{Cp}^*\text{Ru}^{\text{II}}$ -catalyzed synthesis of dihydrobenzoindoles and benzonorcaradienes.

plexes often follow different reaction mechanisms displaying unique reactivity and selectivity. In particular, enantioselective C–H functionalizations with abundant 3d metals remain a challenging research area.^[123,124] Pioneered by Kanai and Matsunaga in 2013,^[125] $\text{Cp}^*\text{Co}^{\text{III}}$ complexes have emerged as powerful catalysts to complement their $\text{Cp}^*\text{Rh}^{\text{III}}$ relatives. Their use in combination with chiral acids has been successful for the induction of enantiocontrol in several different transformations.^[9] Recently, the first example of a $\text{Cp}^*\text{Co}^{\text{III}}$ -catalyzed transformation has been disclosed,^[58] which opens new opportunities for sustainable asymmetric catalyses controlled by chiral Cp^* ligands.

In 2019, the Cramer group reported the development of novel chiral $\text{Cp}^*\text{Co}^{\text{III}}$ complexes and demonstrated their high catalytic efficiency in the C–H functionalization of *N*-chlorobenzamides **256** with alkenes **257** (Scheme 46).^[58] This [4+2] annulation reaction to dihydroisoquinolinones **258** became a benchmark transformation for $\text{Cp}^*\text{Rh}^{\text{III}}$ catalysts (Scheme 17). Among several tested chiral ligands, the BINOL-derivative bearing a *tert*-butyl substituent at the Cp ring (**Co2**) was clearly superior, providing 99% enantiomeric excess in the coupling of *N*-chlorobenzamide **256** ($\text{R} = \text{H}$) and styrene. In comparison, the highest selectivity obtained by Rh^{III} catalysis is 92% *ee*. Several other challenging olefin acceptors **257** were successful. For instance, alkyl olefins, which gave poor enantioselectivities with Cp^*Rh catalysts, afforded dihydroquinolinone derivatives





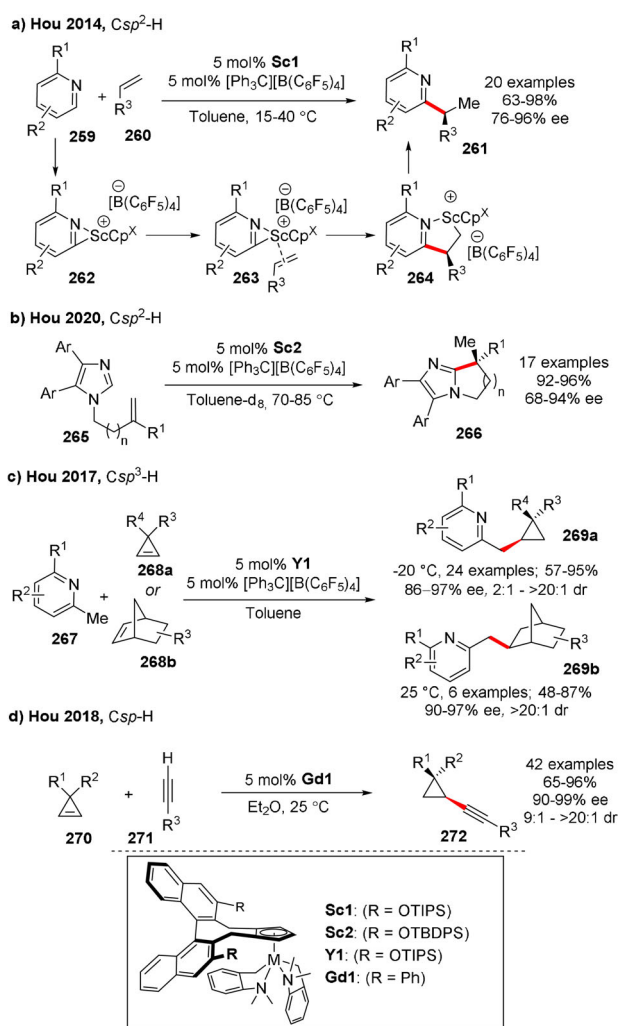
Scheme 46. Co^{III}-catalyzed synthesis of dihydroisoquinolinones via [4+2] annulation of *N*-chlorobenzamides with alkenes.

258 in up to 92% *ee*. Importantly, opposite regiocontrol was observed compared to bulky achiral CpRh^{III} catalysts.^[126–128]

To rationalize the difference in catalyst performance, the authors compared different steric parameters of the Cp^XCo^{III} complexes (Scheme 46, bottom). An important factor is the influence of the distal substituents of the Cp ring on the dihedral angle θ of the biaryl backbone of Cp^X. X-ray analysis revealed that the optimal **Co2** has a larger dihedral angle than **Co1** (76.5° vs. 69.6°), showing a wider opening of the methoxy naphthyl portion from the catalytic pocket. In addition, the CO ligand of **Co2** swapped position with an iodide, indicating a significantly different chiral environment provided by the bulky *tert*-butyl substituted ligand. Steric mapping of the complexes^[129] showed that the naphthyl backbone (backwall in Scheme 2) generates significant bulk in the SW quadrant. In the case of **Co2**, the map shows the great bulk of the *tert*-butyl group, which hinders the southern hemisphere and thereby favors entrance from the north. Hence, while the binaphthyl backwall is responsible for the selective alignment of the metalocycle resulting from C–H activation, the *tert*-butyl group dictates the approach of the incoming alkene substrate.

4.6. Rare-Earth Metal-Catalysis

The natural abundance and unique reactivity of rare-earth metals make them highly attractive. In general, they have a stronger Lewis acid character than transition metals.^[130] Until the early 2010s, half-sandwich complexes of rare-earth metals were most known to catalyze alkene polymerizations. In 2014, the Hou group extended their reactivity to the pyridyl-directed functionalization of C–H bonds (Scheme 47 a).^[57] They employed the BINOL-Cp **Sc1** pre-catalyst to selectively alkylate pyridines **259** with alkenes **260**. Branched products **261** were accessed in good yields and high enantioselectivities, forming a new C(sp²)–C(sp³) bond. Mechanistically, the authors proposed that pyridine coordination to the metal directs C–H activation *ortho* to the nitrogen atom, generating a η^2 -heterocyclic complex **262**. Diastereoselective coordination of the olefin partner con-



Scheme 47. Enantioselective C–C bond formation catalyzed by Cp^X rare-earth metal complexes.

trolled by the chiral Cp ligand (**263**), and migratory insertion lead to a 5-membered metalocycle **264**, creating the carbon stereocenter. Finally, C–H deprotonation of a second molecule of pyridine substrate liberates the product and regenerates the catalyst.

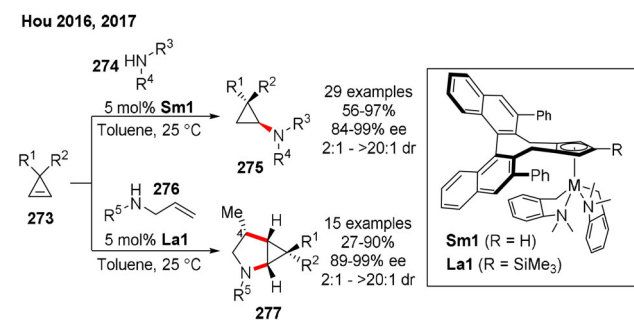
Additional mechanistically related C–C bond forming transformations were developed later by the same group. *N*-substituted imidazoles **265** were shown to react with internal 1,1-disubstituted olefins, generating C-quaternary stereocenters in high enantioselectivity (Scheme 47 b).^[67] Pre-catalyst **Sc2**, bearing bulky silyl ether substituents in the ligand backbone, ensured excellent levels of enantioselectivity toward differently functionalized fused imidazoles **266**. The reaction scope was extended to pyridine benzylic C–H bond addition (**267**) onto strained alkenes **268** (Scheme 47 c).^[66] Remarkably, the choice of the metal had a significant impact on the reaction. While **Y1** gave satisfactory results, the previously successful **Sc1** analog was inactive. Additional factors, such as the BINOL-Cp^X ligand's *ortho* substitution (Ph vs. OTIPS) and the reaction temperature (r.t. to –20 °C), were key for stereocontrol. Several chiral cyclopropanes **269 a**

were accessed with varying levels of diastereoselectivity and with excellent enantioselectivity. Noteworthy, the reaction scope is limited to 2,6-disubstituted aza-arenes **267** ($R^1 \neq H$).

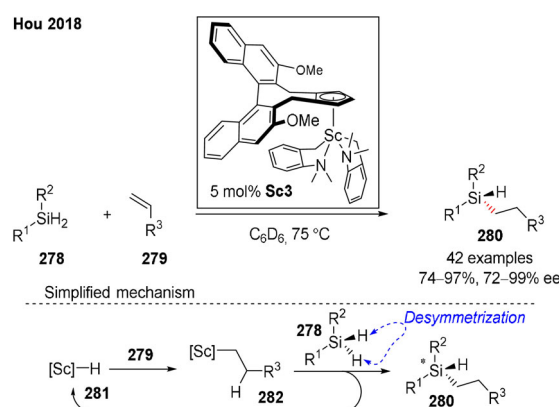
In 2018, Hou and co-workers reported an enantio- and diastereoselective addition of alkynes **271** to cyclopropenes **270** catalyzed by complex **Gd1** (Scheme 47 d).^[131] In the absence of an aza-directing group, the authors proposed that both cyclometalated amine ligands are displaced by two terminal alkyne substrates **271** through an acid–base reaction, generating the catalytically active species (see Scheme 15). An evaluation of different Cp^X metal complexes revealed a big impact of the metal ion size on the reactivity. Compared to Gd^{III} (radius = 0.938 Å), the larger Sm^{III} (0.958 Å) and the smaller Y^{III} (0.900 Å) were less efficient. The significantly smaller Sc^{III} (0.745 Å) failed to provide any desired product.

Cp^X complexes of rare-earth metals have also been successful in the asymmetric construction of C–N bonds. In particular, challenging intermolecular hydroaminations remain underexplored. Notably, the use of Cp^XSm1 enabled the first enantioselective hydroamination of cyclopropenes **273** with secondary amines **274** (Scheme 48),^[132] providing valuable aminocyclopropanes **275** with excellent stereoselectivity (up to 98% *ee* and >20:1 dr). The reaction scope was extended to *N*-allylamines **276**, generating cyclopropane-fused pyrrolidines **277** via carboamination/annulation (Scheme 48).^[133] Whereas **Sm1** provided high enantioselectivity (90% *ee*), no diastereocontrol was observed at the C4 position. Metal Cp^X ligand optimization studies showed that Cp^XLa1 , bearing a third substituent at the Cp ring, led to increased diastereo- and enantioselectivity (99% *ee* and 15:1 dr). Noteworthy, the opposite C4 epimer was favored when using a Cp^X -disubstituted La complex.

Complementary to Cp^XRh and Cp^XIr catalysts for the synthesis of chiral-at-P or -S compounds (Sections 4.2 and 4.3, respectively), Cp^XSc complexes are efficient catalysts for the asymmetric construction of silicon-stereogenic molecules. Despite the importance of these compounds in organic synthesis and drug discovery,^[134] their enantioselective synthesis remains elusive.^[135] In 2018, Hou et al. reported a hydrosilylation of terminal olefins **279** with prochiral dihydrosilanes **278**, affording differently functionalized chiral silanes **280** (Scheme 49).^[136] Mechanistically, the authors propose a metal hydride species as the active catalyst (**281**), formed in situ from pre-catalyst **Sc3** and dihydrosilane



Scheme 48. Enantioselective C–N bond formation catalyzed by Cp^X rare-earth metal complexes.



Scheme 49. $ScCp^X$ -catalyzed enantioselective Si–C bond formation by desymmetrization.

278. Subsequent regioselective hydrometalation of the C–C double bond generates the linear organoscandium intermediate **282**. Finally, enantioselective dihydrosilane alkylation by σ -bond metathesis forms the silicon chiral center (**280**) and regenerates the active metal hydride species **281**.

5. Summary and Outlook

Chiral cyclopentadienyls (Cp^X) have emerged as powerful stereocontrolling ligands in asymmetric metal catalysis. Triggered by two independent reports in 2012 by Cramer^[38] and Ward and Rovis^[40] on Cp^XRh^{III} -catalyzed enantioselective C–H functionalization, an impressive number of half-sandwich Cp^X metal complexes have been demonstrated to effectively catalyze mechanistically diverse transformations, giving access to an extensive catalogue of optically enriched molecules. Currently, the state of this art goes far beyond the proof of principle. Several different Cp^X ligand classes have been developed, which rely on central, axial, planar, and macromolecular chirality. Among them, the atropochiral binaphthyl-derived scaffold has been undoubtedly the most predominant, complexed to transition metals (Rh, Ir, Ru, Co) as well as rare-earth metals (Sc, Y, La, Sm, Gd, ...). Nevertheless, research into modular and even more efficient platforms must persist, as no ligand will be universally suitable.

Future additional efforts should focus on rationalizing the selectivity-determining features of the Cp^X metal complexes. Currently, the ligand screening for reaction optimization purposes is based on the chemist's intuition, and the application of systematic structural modifications on the best hit is time-consuming. In order to expedite this process, not only more efficient shorter ligand synthesis are needed, but their stereoelectronic parametrization for modern computer-based predictive tools should be considered as well.^[137] In line with this, further development of ligand complexation methods allowing the in situ formation of the active metal complex^[59,138] is essential for their incorporation in rapid catalyst screening setups. Commercialization of the chiral diene pre-ligands would also facilitate their access to non-specialized academic research labs and industries.



With the urge for sustainable chemical processes, more importance should be given to Cp^X complexes of abundant first-row transition metals, which have recently emerged as alternatives to precious metals.^[58,124] The application of energies such as electricity may be beneficial for catalyst activation, for instance, replacing stoichiometric chemical oxidants.^[139] Irradiation with light may also unlock new reactivities.^[140,141] Recycling of the metal complexes would also be highly desirable, as well as the capability of maintaining high efficiencies in green solvents or even living cells and organisms. We hope this Review will inspire future research efforts to reveal the full power of chiral Cp^X ligands in catalysis.

Acknowledgements

This work is supported by the EPFL and the Swiss National Science Foundation (no 157741).

Conflict of interest

The authors declare no conflict of interest.

- [1] A. Calcaterra, I. D'Acquarica, *J. Pharm. Biomed. Anal.* **2018**, *147*, 323–340.
- [2] H.-U. Blaser, H.-J. Federsel in *Asymmetric Catalysis on Industrial Scale: Challenges, Approaches and Solutions*, Wiley-VCH, Weinheim, **2010**.
- [3] T. P. Yoon, E. N. Jacobsen, *Science* **2003**, *299*, 1691–1693.
- [4] Q.-L. Zhou in *Privileged Chiral Ligands and Catalysts*, Wiley-VCH, Weinheim, **2011**.
- [5] D. Janssen-Müller, C. Schlepphorst, F. Glorius, *Chem. Soc. Rev.* **2017**, *46*, 4845–4854.
- [6] R. L. Halterman, *Chem. Rev.* **1992**, *92*, 965–994.
- [7] B. Ye, N. Cramer, *Acc. Chem. Res.* **2015**, *48*, 1308–1318.
- [8] C. G. Newton, D. Kossler, N. Cramer, *J. Am. Chem. Soc.* **2016**, *138*, 3935–3941.
- [9] a) T. Yoshino, S. Satake, S. Matsunaga, *Chem. Eur. J.* **2020**, *26*, 7346–7357; b) F. Pescioli, U. Dhawa, J. C. A. Oliveira, R. Yin, M. John, L. Ackermann, *Angew. Chem. Int. Ed.* **2018**, *57*, 15425–15429; *Angew. Chem.* **2018**, *130*, 15651–15655; c) S. Fukagawa, Y. Kato, R. Tanaka, M. Kojima, T. Yoshino, S. Matsunaga, *Angew. Chem. Int. Ed.* **2019**, *58*, 1153–1157; *Angew. Chem.* **2019**, *131*, 1165–1169.
- [10] T. J. Kealy, P. L. Pauson, *Nature* **1951**, *168*, 1039–1040.
- [11] P. Jutz, N. Burford, *Chem. Rev.* **1999**, *99*, 969–990.
- [12] S. Arndt, J. Okuda, *Chem. Rev.* **2002**, *102*, 1953–1976.
- [13] R. H. Crabtree in *The Organometallic Chemistry of the Transition Metals*, Wiley, **2014**.
- [14] W. J. Evans, *Organometallics* **2016**, *35*, 3088–3100.
- [15] C. Elschenbroich in *Organometallics 3rd ed.* Wiley-VCH, Weinheim, **2006**.
- [16] J. Hartwig in *Organotransition Metal Chemistry: From Bonding to Catalysis*, University Science Books, Sausalito, **2010**.
- [17] M. J. Calhorda, L. F. Veiros, *Comments Inorg. Chem.* **2001**, *22*, 375–391.
- [18] C. Janiak, U. Versteeg, K. C. H. Lange, R. Weimann, E. Hahn, *J. Organomet. Chem.* **1995**, *501*, 219–234.
- [19] N. Dunwoody, S.-S. Sun, A. J. Lees, *Inorg. Chem.* **2000**, *39*, 4442–4451.
- [20] T. Piou, F. Romanov-Michailidis, M. Romanova-Michaelides, K. E. Jackson, N. Semakul, T. D. Taggart, B. S. Newell, C. D. Rithner, R. S. Paton, T. Rovis, *J. Am. Chem. Soc.* **2017**, *139*, 1296–1310.
- [21] T. Piou, T. Rovis, *Acc. Chem. Res.* **2018**, *51*, 170–180.
- [22] R. B. King, M. B. Bisnette, *J. Organomet. Chem.* **1967**, *8*, 287–297.
- [23] J. Okuda in *Transition metal complexes of sterically demanding cyclopentadienyl ligands* (Eds.: W. A. Herrmann); Topics in Current Chemistry, Springer, Berlin, **1992**, pp. 97–145.
- [24] R. Benn, H. Grondey, G. Erker, R. Aul, R. Nolte, *Organometallics* **1990**, *9*, 2493–2497.
- [25] L.-X. Dai, X.-L. Hou in *Chiral Ferrocenes in Asymmetric Catalysis*, Wiley-VCH, Weinheim, **2010**.
- [26] H.-U. Blaser, B. Pugin, F. Spindler, E. Mejía, A. Togni in *Privileged Chiral Ligands and Catalysts* (Eds.: Q.-L. Zhou), Wiley-VCH, Weinheim, **2011**, Chapter 3.
- [27] A. H. Hoveyda, J. P. Morken, *Angew. Chem. Int. Ed. Engl.* **1996**, *35*, 1262–1284; *Angew. Chem.* **1996**, *108*, 1378–1401.
- [28] E. P. Kündig, C. M. Saudan, F. Viton, *Adv. Synth. Catal.* **2001**, *343*, 51–56.
- [29] K. Murata, T. Ikariya, R. Noyori, *J. Org. Chem.* **1999**, *64*, 2186–2187.
- [30] H. Wang, Y. Park, Z. Bai, S. Chang, G. He, G. Chen, *J. Am. Chem. Soc.* **2019**, *141*, 7194–7201.
- [31] Y. Matsushima, K. Onitsuka, T. Kondo, T. Mitsudo, S. Takahashi, *J. Am. Chem. Soc.* **2001**, *123*, 10405–10406.
- [32] B. M. Trost, M. Rao, A. P. Dieskau, *J. Am. Chem. Soc.* **2013**, *135*, 18697–18704.
- [33] E. Cesarotti, H. B. Kagan, R. Goddard, C. Krüger, *J. Organomet. Chem.* **1978**, *162*, 297–309.
- [34] E. Cesarotti, R. Ugo, H. B. Kagan, *Angew. Chem. Int. Ed. Engl.* **1979**, *18*, 779–780; *Angew. Chem.* **1979**, *91*, 842–843.
- [35] R. L. Halterman, K. P. C. Vollhardt, *Tetrahedron Lett.* **1986**, *27*, 1461–1464.
- [36] R. L. Halterman, K. P. C. Vollhardt, *Organometallics* **1988**, *7*, 883–892.
- [37] S. L. Colletti, R. L. Halterman, *Tetrahedron Lett.* **1989**, *30*, 3513–3516.
- [38] B. Ye, N. Cramer, *Science* **2012**, *338*, 504–506.
- [39] B. Ye, N. Cramer, *J. Am. Chem. Soc.* **2013**, *135*, 636–639.
- [40] T. K. Hyster, L. Knorr, T. R. Ward, T. Rovis, *Science* **2012**, *338*, 500–503.
- [41] Y. Sun, N. Cramer, *Chem. Sci.* **2018**, *9*, 2981–2985.
- [42] W.-J. Cui, Z.-J. Wu, Q. Gu, S.-L. You, *J. Am. Chem. Soc.* **2020**, *142*, 7379–7385.
- [43] S. Reddy Chidipudi, D. J. Burns, I. Khan, H. W. Lam, *Angew. Chem. Int. Ed.* **2015**, *54*, 13975–13979; *Angew. Chem.* **2015**, *127*, 14181–14185.
- [44] C. Duchemin, G. Smits, N. Cramer, *Organometallics* **2019**, *38*, 3939–3947.
- [45] J. Zheng, W.-J. Cui, C. Zheng, S.-L. You, *J. Am. Chem. Soc.* **2016**, *138*, 5242–5245.
- [46] Z.-J. Jia, C. Merten, R. Gontla, C. G. Daniliuc, A. P. Antonchick, H. Waldmann, *Angew. Chem. Int. Ed.* **2017**, *56*, 2429–2434; *Angew. Chem.* **2017**, *129*, 2469–2474.
- [47] a) S.-G. Wang, S. H. Park, N. Cramer, *Angew. Chem. Int. Ed.* **2018**, *57*, 5459–5462; *Angew. Chem.* **2018**, *130*, 5557–5560; b) H. Liang, L. Vasamsetty, T. Li, J. Jiang, X. Pang, J. Wang, *Chem. Eur. J.* **2020**, <https://doi.org/10.1002/chem.202001814>.
- [48] W. Li, Z. Zhang, D. Xiao, X. Zhang, *J. Org. Chem.* **2000**, *65*, 3489–3496.
- [49] B. Ye, N. Cramer, *Synlett* **2015**, *26*, 1490–1495.
- [50] T. Ooi, M. Kameda, K. Maruoka, *J. Am. Chem. Soc.* **2003**, *125*, 5139–5151.
- [51] D. Kossler, N. Cramer, *J. Am. Chem. Soc.* **2015**, *137*, 12478–12481.



- [52] S.-F. Zhu, Y. Yang, L.-X. Wang, B. Liu, Q.-L. Zhou, *Org. Lett.* **2005**, *7*, 2333–2335.
- [53] H. Gotoh, H. Ogino, H. Ishikawa, Y. Hayashi, *Tetrahedron* **2010**, *66*, 4894–4899.
- [54] G. Erker, A. A. H. van der Zeijden, *Angew. Chem. Int. Ed. Engl.* **1990**, *29*, 512–514; *Angew. Chem.* **1990**, *102*, 543–545.
- [55] a) A. Gutnov, B. Heller, C. Fischer, H.-J. Drexler, A. Spannenberg, B. Sundermann, C. Sundermann, *Angew. Chem. Int. Ed.* **2004**, *43*, 3795–3797; *Angew. Chem.* **2004**, *116*, 3883–3886; b) P. Jungk, T. Täufer, I. Thiel, M. Hapke, *Synthesis* **2016**, *48*, 2026–2035.
- [56] M. Dieckmann, Y.-S. Jang, N. Cramer, *Angew. Chem. Int. Ed.* **2015**, *54*, 12149–12152; *Angew. Chem.* **2015**, *127*, 12317–12320.
- [57] G. Song, W. W. N. O, Z. Hou, *J. Am. Chem. Soc.* **2014**, *136*, 12209–12212.
- [58] K. Ozols, Y.-S. Jang, N. Cramer, *J. Am. Chem. Soc.* **2019**, *141*, 5675–5680.
- [59] B. Audic, M. D. Wodrich, N. Cramer, *Chem. Sci.* **2019**, *10*, 781–787.
- [60] M. Brauns, N. Cramer, *Angew. Chem. Int. Ed.* **2019**, *58*, 8902–8906; *Angew. Chem.* **2019**, *131*, 8994–8998.
- [61] T. J. Potter, D. N. Kamber, B. Q. Mercado, J. A. Ellman, *ACS Catal.* **2017**, *7*, 150–153.
- [62] X. Chen, S. Yang, H. Li, B. Wang, G. Song, *ACS Catal.* **2017**, *7*, 2392–2396.
- [63] T. Reiner, D. Jantke, A. Raba, A. N. Marziale, J. Eppinger, *J. Organomet. Chem.* **2009**, *694*, 1934–1937.
- [64] E. A. Trifonova, N. M. Ankudinov, A. A. Mikhaylov, D. A. Chusov, Y. V. Nelyubina, D. S. Perekalin, *Angew. Chem. Int. Ed.* **2018**, *57*, 7714–7718; *Angew. Chem.* **2018**, *130*, 7840–7844.
- [65] a) X. Yan, P. Zhao, H. Liang, H. Xie, J. Jiang, S. Gou, J. Wang, *Org. Lett.* **2020**, *22*, 3219–3223; b) S. Satake, T. Kurihara, K. Nishikawa, T. Mochizuki, M. Hatano, K. Ishihara, T. Yoshino, S. Matsunaga, *Nat. Catal.* **2018**, *1*, 585–591.
- [66] Y. Luo, H.-L. Teng, M. Nishiura, Z. Hou, *Angew. Chem. Int. Ed.* **2017**, *56*, 9207–9210; *Angew. Chem.* **2017**, *129*, 9335–9338.
- [67] S.-J. Lou, Z. Mo, M. Nishiura, Z. Hou, *J. Am. Chem. Soc.* **2020**, *142*, 1200–1205.
- [68] B. Heller, A. Gutnov, C. Fischer, H.-J. Drexler, A. Spannenberg, D. Redkin, C. Sundermann, B. Sundermann, *Chem. Eur. J.* **2007**, *13*, 1117–1128.
- [69] L. Ackermann, *Chem. Rev.* **2011**, *111*, 1315–1345.
- [70] I. S. Hassan, A. N. Ta, M. W. Danneman, N. Semakul, M. Burns, C. H. Basch, V. N. Dippon, B. R. McNaughton, T. Rovis, *J. Am. Chem. Soc.* **2019**, *141*, 4815–4819.
- [71] C. G. Newton, N. Cramer in *Rhodium Catal. Org. Synth.*, Wiley-VCH, Weinheim, **2019**, pp. 629–644.
- [72] B. Ye, P. A. Donets, N. Cramer, *Angew. Chem. Int. Ed.* **2014**, *53*, 507–511; *Angew. Chem.* **2014**, *126*, 517–521.
- [73] W. Chen, J. Li, H. Xie, J. Wang, *Org. Lett.* **2020**, *22*, 3586–3590.
- [74] S. Maity, T. J. Potter, J. A. Ellman, *Nat. Catal.* **2019**, *2*, 756–762.
- [75] T. Piou, T. Rovis, *J. Am. Chem. Soc.* **2014**, *136*, 11292–11295.
- [76] C. Duchemin, N. Cramer, *Chem. Sci.* **2019**, *10*, 2773–2777.
- [77] C. Duchemin, N. Cramer, *Angew. Chem. Int. Ed.* **2020**, <https://doi.org/10.1002/anie.202006149>; *Angew. Chem.* **2020**, <https://doi.org/10.1002/ange.202006149>.
- [78] G. Zheng, Z. Zhou, G. Zhu, S. Zhai, H. Xu, X. Duan, W. Yi, X. Li, *Angew. Chem. Int. Ed.* **2020**, *59*, 2890–2896; *Angew. Chem.* **2020**, *132*, 2912–2918.
- [79] S.-G. Wang, N. Cramer, *Angew. Chem. Int. Ed.* **2019**, *58*, 2514–2518; *Angew. Chem.* **2019**, *131*, 2536–2540.
- [80] X. Yang, G. Zheng, X. Li, *Angew. Chem. Int. Ed.* **2019**, *58*, 322–326; *Angew. Chem.* **2019**, *131*, 328–332.
- [81] R. Mi, G. Zheng, Z. Qi, X. Li, *Angew. Chem. Int. Ed.* **2019**, *58*, 17666–17670; *Angew. Chem.* **2019**, *131*, 17830–17834.
- [82] B. Ye, N. Cramer, *Angew. Chem. Int. Ed.* **2014**, *53*, 7896–7899; *Angew. Chem.* **2014**, *126*, 8030–8033.
- [83] T. Li, C. Zhou, X. Yan, J. Wang, *Angew. Chem. Int. Ed.* **2018**, *57*, 4048–4052; *Angew. Chem.* **2018**, *130*, 4112–4116.
- [84] a) S.-G. Wang, Y. Liu, N. Cramer, *Angew. Chem. Int. Ed.* **2019**, *58*, 18136–18140; *Angew. Chem.* **2019**, *131*, 18304–18308; b) S.-G. Wang, N. Cramer, *ACS Catal.* **2020**, *10*, 8231–8236.
- [85] A. Ding, M. Meazza, H. Guo, J. W. Yang, R. Rios, *Chem. Soc. Rev.* **2018**, *47*, 5946–5996.
- [86] J. Zheng, S.-B. Wang, C. Zheng, S.-L. You, *J. Am. Chem. Soc.* **2015**, *137*, 4880–4883.
- [87] C. Zheng, J. Zheng, S.-L. You, *ACS Catal.* **2016**, *6*, 262–271.
- [88] M. V. Pham, N. Cramer, *Chem. Eur. J.* **2016**, *22*, 2270–2273.
- [89] J. Zheng, S.-B. Wang, C. Zheng, S.-L. You, *Angew. Chem. Int. Ed.* **2017**, *56*, 4540–4544; *Angew. Chem.* **2017**, *129*, 4611–4615.
- [90] H. Li, R. Gontla, J. Flegel, C. Merten, S. Ziegler, A. P. Antonchick, H. Waldmann, *Angew. Chem. Int. Ed.* **2019**, *58*, 307–311; *Angew. Chem.* **2019**, *131*, 313–317.
- [91] L. Kong, X. Han, S. Liu, Y. Zou, Y. Lan, X. Li, *Angew. Chem. Int. Ed.* **2020**, *59*, 7188–7192; *Angew. Chem.* **2020**, *132*, 7255–7259.
- [92] G. Liao, T. Zhou, Q.-J. Yao, B.-F. Shi, *Chem. Commun.* **2019**, *55*, 8514–8523.
- [93] J. Zheng, S.-L. You, *Angew. Chem. Int. Ed.* **2014**, *53*, 13244–13247; *Angew. Chem.* **2014**, *126*, 13460–13463.
- [94] a) G. Shan, J. Flegel, H. Li, C. Merten, S. Ziegler, A. P. Antonchick, H. Waldmann, *Angew. Chem. Int. Ed.* **2018**, *57*, 14250–14254; *Angew. Chem.* **2018**, *130*, 14446–14450; b) H. Li, X. Yan, J. Zhang, W. Guo, J. Jiang, J. Wang, *Angew. Chem. Int. Ed.* **2019**, *58*, 6732–6736; *Angew. Chem.* **2019**, *131*, 6804–6808.
- [95] M. Tian, D. Bai, G. Zheng, J. Chang, X. Li, *J. Am. Chem. Soc.* **2019**, *141*, 9527–9532.
- [96] F. Wang, Z. Qi, Y. Zhao, S. Zhai, G. Zheng, R. Mi, Z. Huang, X. Zhu, X. He, X. Li, *Angew. Chem. Int. Ed.* **2020**, <https://doi.org/10.1002/anie.202002208>; *Angew. Chem.* **2020**, <https://doi.org/10.1002/ange.202002208>.
- [97] S.-B. Wang, J. Zheng, S.-L. You, *Organometallics* **2016**, *35*, 1420–1425.
- [98] S.-B. Wang, Q. Gu, S.-L. You, *Organometallics* **2017**, *36*, 4359–4362.
- [99] J. Diesel, N. Cramer, *ACS Catal.* **2019**, *9*, 9164–9177.
- [100] M. Dutartre, J. Bayardon, S. Jugé, *Chem. Soc. Rev.* **2016**, *45*, 5771–5794.
- [101] J. A. Sirvent, U. Lücking, *ChemMedChem* **2017**, *12*, 487–501.
- [102] Y. Sun, N. Cramer, *Angew. Chem. Int. Ed.* **2017**, *56*, 364–367; *Angew. Chem.* **2017**, *129*, 370–373.
- [103] Y. Sun, N. Cramer, *Angew. Chem. Int. Ed.* **2018**, *57*, 15539–15543; *Angew. Chem.* **2018**, *130*, 15765–15769.
- [104] B. Shen, B. Wan, X. Li, *Angew. Chem. Int. Ed.* **2018**, *57*, 15534–15538; *Angew. Chem.* **2018**, *130*, 15760–15764.
- [105] L. Lin, S. Fukagawa, D. Sekine, E. Tomita, T. Yoshino, S. Matsunaga, *Angew. Chem. Int. Ed.* **2018**, *57*, 12048–12052; *Angew. Chem.* **2018**, *130*, 12224–12228.
- [106] S. Fukagawa, M. Kojima, T. Yoshino, S. Matsunaga, *Angew. Chem. Int. Ed.* **2019**, *58*, 18154–18158; *Angew. Chem.* **2019**, *131*, 18322–18326.
- [107] D. Gwon, S. Park, S. Chang, *Tetrahedron* **2015**, *71*, 4504–4511.
- [108] Y.-S. Jang, M. Dieckmann, N. Cramer, *Angew. Chem. Int. Ed.* **2017**, *56*, 15088–15092; *Angew. Chem.* **2017**, *129*, 15284–15288.
- [109] Y.-S. Jang, Ł. Woźniak, J. Pedroni, N. Cramer, *Angew. Chem. Int. Ed.* **2018**, *57*, 12901–12905; *Angew. Chem.* **2018**, *130*, 13083–13087.
- [110] A. Fürstner, F. Stelzer, H. Szillat, *J. Am. Chem. Soc.* **2001**, *123*, 11863–11869.
- [111] D. J. Ager, A. H. M. de Vries, J. G. de Vries, *Chem. Soc. Rev.* **2012**, *41*, 3340–3380.



- [112] J. M. Zimbron, T. Heinisch, M. Schmid, D. Hamels, E. S. Nogueira, T. Schirmer, T. R. Ward, *J. Am. Chem. Soc.* **2013**, *135*, 5384–5388.
- [113] J. Mas-Roselló, T. Smejkal, N. Cramer, *Science* **2020**, *368*, 1098–1102.
- [114] O. Eisenstein, R. H. Crabtree, *New J. Chem.* **2013**, *37*, 21–27.
- [115] B. M. Trost, M. U. Frederiksen, M. T. Rudd, *Angew. Chem. Int. Ed.* **2005**, *44*, 6630–6666; *Angew. Chem.* **2005**, *117*, 6788–6825.
- [116] B. M. Trost, F. D. Toste, A. B. Pinkerton, *Chem. Rev.* **2001**, *101*, 2067–2096.
- [117] D. Kossler, N. Cramer, *Chim. Int. J. Chem.* **2017**, *71*, 186–189.
- [118] D. Kossler, N. Cramer, *Chem. Sci.* **2017**, *8*, 1862–1866.
- [119] T. Mitsudo, H. Naruse, T. Kondo, Y. Ozaki, Y. Watanabe, *Angew. Chem. Int. Ed. Engl.* **1994**, *33*, 580–581; *Angew. Chem.* **1994**, *106*, 595–597.
- [120] D. Kossler, F. G. Perrin, A. A. Suleymanov, G. Kiefer, R. Scopelliti, K. Severin, N. Cramer, *Angew. Chem. Int. Ed.* **2017**, *56*, 11490–11493; *Angew. Chem.* **2017**, *129*, 11648–11651.
- [121] S. H. Park, S.-G. Wang, N. Cramer, *ACS Catal.* **2019**, *9*, 10226–10231.
- [122] P. Gandeepan, T. Müller, D. Zell, G. Cera, S. Warratz, L. Ackermann, *Chem. Rev.* **2019**, *119*, 2192–2452.
- [123] J. Loup, U. Dhawa, F. Pesciaoli, J. Wencel-Delord, L. Ackermann, *Angew. Chem. Int. Ed.* **2019**, *58*, 12803–12818; *Angew. Chem.* **2019**, *131*, 12934–12949.
- [124] Ł. Woźniak, N. Cramer, *Trends Chem.* **2019**, *1*, 471–484.
- [125] T. Yoshino, H. Ikemoto, S. Matsunaga, M. Kanai, *Angew. Chem. Int. Ed.* **2013**, *52*, 2207–2211; *Angew. Chem.* **2013**, *125*, 2263–2267.
- [126] T. K. Hyster, D. M. Dalton, T. Rovis, *Chem. Sci.* **2015**, *6*, 254–258.
- [127] T. K. Hyster, D. M. Dalton, T. Rovis, *Chem. Sci.* **2017**, *8*, 1666.
- [128] E. A. Trifonova, N. M. Ankudinov, M. V. Kozlov, M. Y. Sharipov, Y. V. Nelyubina, D. S. Perekalin, *Chem. Eur. J.* **2018**, *24*, 16570–16575.
- [129] A. Poater, B. Cosenza, A. Correa, S. Giudice, F. Ragone, V. Scarano, L. Cavallo, *Eur. J. Inorg. Chem.* **2009**, 1759–1766.
- [130] M. Nishiura, F. Guo, Z. Hou, *Acc. Chem. Res.* **2015**, *48*, 2209–2220.
- [131] H.-L. Teng, Y. Ma, G. Zhan, M. Nishiura, Z. Hou, *ACS Catal.* **2018**, *8*, 4705–4709.
- [132] H.-L. Teng, Y. Luo, B. Wang, L. Zhang, M. Nishiura, Z. Hou, *Angew. Chem. Int. Ed.* **2016**, *55*, 15406–15410; *Angew. Chem.* **2016**, *128*, 15632–15636.
- [133] H.-L. Teng, Y. Luo, M. Nishiura, Z. Hou, *J. Am. Chem. Soc.* **2017**, *139*, 16506–16509.
- [134] J. S. Mills, G. A. Showell, *Expert Opin. Invest. Drugs* **2004**, *13*, 1149–1157.
- [135] L.-W. Xu, L. Li, G.-Q. Lai, J.-X. Jiang, *Chem. Soc. Rev.* **2011**, *40*, 1777–1790.
- [136] G. Zhan, H.-L. Teng, Y. Luo, S.-J. Lou, M. Nishiura, Z. Hou, *Angew. Chem. Int. Ed.* **2018**, *57*, 12342–12346; *Angew. Chem.* **2018**, *130*, 12522–12526.
- [137] A. F. Zahrt, S. V. Athavale, S. E. Denmark, *Chem. Rev.* **2020**, *120*, 1620–1689.
- [138] G. Smits, B. Audic, M. D. Wodrich, C. Corminboeuf, N. Cramer, *Chem. Sci.* **2017**, *8*, 7174–7179.
- [139] T. H. Meyer, L. H. Finger, P. Gandeepan, L. Ackermann, *Trends Chem.* **2019**, *1*, 63–76.
- [140] S. M. Barrett, C. L. Pitman, A. G. Walden, A. J. M. Miller, *J. Am. Chem. Soc.* **2014**, *136*, 14718–14721.
- [141] P. Gandeepan, J. Koeller, K. Korvorapun, J. Mohr, L. Ackermann, *Angew. Chem. Int. Ed.* **2019**, *58*, 9820–9825; *Angew. Chem.* **2019**, *131*, 9925–9930.

Manuscript received: June 8, 2020

Accepted manuscript online: July 16, 2020

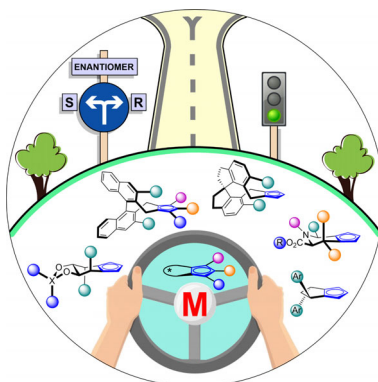
Version of record online: ■ ■ ■ ■ ■ ■ ■ ■ ■ ■

Reviews

Cyclopentadienyl Ligands

J. Mas-Roselló, A. G. Herraiz, B. Audic,
A. Laverny, N. Cramer* — ■■■—■■■

Chiral Cyclopentadienyl Ligands: Design,
Syntheses, and Applications in
Asymmetric Catalysis



Chiral cyclopentadienyls (Cp^x) have emerged as powerful steering ligands in asymmetric catalysis. This Review discusses the existing ligand classes, their design, syntheses, and metalation methods. Details on the successful application of the metal complexes in numerous catalytic processes are provided. Those include C–H bond functionalization chemistry and beyond, enabling access to valuable chiral molecules.